PŘÍRODOVĚDECKÁ FAKULTA UNIVERZITY KARLOVY
ÚSTAV GEOLOGIE A PALEONTOLOGIE

Subdukcí řízené zkrácení a diferenciální exhumace v kadomském akrečním klínu tepelsko–barrandienské jednotky (Český masív)

Subduction-driven shortening and differential exhumation in a Cadomian accretionary wedge: The Teplá–Barrandian unit, Bohemian Massif

Rigorózní práce

Mgr. Jaroslava Hajná

Vedoucí rigorózní práce: RNDr. Jiří Žák, Ph.D.

Praha 2010

Obsah

Prohlašuji, že jsem na této rigorózní práci pracovala samostatně za pomoci mého školitele a všechny použité prameny jsem řádně citovala.

.....

Svoluji k zapůjčení této rigorózní práce ke studijním účelům, žádám o vedení evidence půjčování a její řádné citování.

Datum	Jméno	Pracoviště	Podpis

1. Abstrakt

Předkládaná rigorózní práce je zaměřena na studium tektonických deformací v neoproterozoických a nadložních spodnopaleozoických horninách tepelsko-barrandienské jednotky (TBJ) podél sz. okraje pražské pánve v centrální části Českého masívu. Hlavním cílem výzkumu bylo odlišit a charakterizovat struktury vzniklé během kadomské a variské orogeneze pomocí moderních metod a srovnáním finitních deformačních struktur v různých geologických jednotkách (neoproterozoikum, spodní paleozoikum). Toto srovnání umožnilo studovat tektonické procesy a přímý záznam deformační historie avalonsko-kadomského orogenního pásma během neoproterozoika a pomohlo dešifrovat strukturní záznam kadomských tektonických procesů ve svrchní kůře peri-gondwanských teránů. Tato práce umožnila novou interpretaci kadomských tektonických deformací v Českém masívu, včetně sukcese jednotlivých deformačních fází, deformačních gradientů a mechanismů deformace. Výsledkem bylo vytvoření celkového tektonického modelu kadomského vývoje a variského přetisku ve východní části tepelsko-barrandienské jednotky a rovněž širší korelace geodynamických procesů v jednotlivých teránech avalonsko-kadomského pásma během Neoproterozoika.

2. English abstract

This doctoral thesis is focused on analysis of tectonic deformations a geodynamic evolution of Neoproterozoic and Lower Paleozoic rocks of the Teplá−Barrandian Unit along the northwestern margin of the Prague basin (central Bohemian Massif). Using a wide range of modern methods, correlation of finite deformation patterns in different units allowed separation of structures formed during Cadomian and Variscan orogeny and interpretation of tectonic processes and tectonic history of the Cadomian orogenic belt during late Neoproterozoic. The research found direct evidence for and enabled new interpretations of Cadomian tectonic processes in the Bohemian Massif, including a succesion of deformation phases, quantification of finite deformation gradients and mechanisms. The different data sets were finally combined into an overall geotectonic model of Cadomian orogeny and its Variscan tectonothermal overprint in the Bohemian Massif, as well as the data were used for correlation with other Avalonian−Cadomian terranes.

3. Úvod

Neoproterozoikum představuje velmi důležitou časovou etapu v historii planety Země, pro kterou jsou charakteristické např. vznik rozsáhlých lineárních orogenních pásem, které se stavbou podobají fanerozoickým orogénům, zásadní změny v geochemii oceánů a složení atmosféry, existence rozsáhlých kontinentálních ledovců a rozvoj nových mnohobuněčných forem života, které předcházely explozivnímu nástupu skeletálních forem organismů na hranici prekambria a kambria.

Klíčovou roli při globálně tektonickém vývoji během neoproterozoika hrál vznik superkontinentu Rodinia v době před cca 1 miliardou let, následovaný jeho rozpadem, který započal před 750 milióny let, a kontinentání tzv. panafrické kolize, během kterých došlo ke spojení východní a západní Gondwany. V severním lemu nově vytvořené Gondwany vzniká systém ostrovních oblouků a zaobloukových pánví, jejichž deformací či kolizemi s gondwanskou pevninou se vytváří v závěru neoproterozoika tzv. avalonsko-kadomský orogén, jehož zbytky můžeme dnes studovat v několika korových segmentech (tzv. alochtonní tektonostratigrafické terány – Florida, Carolina, Avalonia, Iberia, Cadomia, Bohemia či Perunica aj.) zapracovaných do mladších orogenních pásem nyní na severní polokouli (Murphy et al., 2002, 2004). Jak naznačují izotopické signatury basementu, tyto některé tzv. perigondwanské terány původně sousedily s amazonským kratonem, zatímco jiné mají afinitu k západoafrickému kratonu (Nance a Murphy, 1994; Nance et al., 2002). Geotektonický vývoj těchto teránů je v současné době interpretován jako výsledek tvorby vulkanických oblouků a dlouhodobé subdukce oceánské kůry pod aktivní kontinentální okraj (severní okraj Gondwany), doprovázené vápenatoalkalickým magmatismem, vznikem zaobloukových pánví na horizontálních posunech a jejich následnou inverzí. Geochronologická data indikují, že počátek subdukce a vápenatoalkalického magmatismu se odehrál mezi 635−620 Ma a k ukončení tektonomagmatické aktivity spjaté se subdukcí

docházelo v širším intervalu 605−570 Ma. Pro další vývoj avalonsko-kadomských teránů je typický přechod od subdukce ke vzniku extenzních a transtenzních intrakontinentálních pánví a klastické kontinentální sedimentaci během spodního kambria. Charakteristickým rysem vývoje perigondwanských teránů je rovněž absence kontinentální kolize a výrazného ztluštění kůry.

Naše současné znalosti o geotektonickém prostředí a vývoji avalonsko-kadomského pásma jsou z velké části založeny na geochronologii a interpretaci (diskriminaci) geochemických dat. Až na vyjímky (např. Ballévre et al., 2001), detailní studie zabývající se hledáním přímých důkazů pro globální tektonické modely (v podobě strukturního záznamu v neoproterozoických horninách) většinou chybí nebo jsou tyto studie komplikovány pozdějším tektonometamorfním přetiskem během mladších geotektonických cyklů. Jeden z nejlépe odkrytých terénů, kde lze studovat tektonické procesy a přímý záznam deformační historie kadomského orogenního pásma během neoproterozoika představuje tepelsko-barrandienská jednotka v centrální části Českého masívu, neboť tato jednotka nebyla výrazně zanořena a metamorfována během variské orogeneze. Tato jednotka tak představuje jeden z nejlépe zachovaných reliktů peri-gondwanských teránů kadomského orogenního pásma.

Tepelsko-barrandienská jednotka představuje svrchněkorový segment v centrální části českého masívu, oklopený na jv., jz. a sz. od výše metamorfovaných jednotek střižnými zónami nebo variskými plutonity. Základ (basement) tepelsko-barrandienské jednotky tvoří horniny neoproterozoika, na které diskordantně nasedají zvrásněné spodnopaleozoické vrstevní sledy.

Podle současné stratigrafické koncepce se dělí neoproterozoikum tepelsko-barrandienské jednotky na dvě skupiny: starší kralupsko-zbraslavskou a mladší štěchovickou. Kralupsko-zbraslavská skupina zahrnuje střídání drob, prachovců, černých břidlic, silicitů a

převážně bazických vulkanitů, zatímco nadložní štěchovická skupina, která vystupuje v jv. křídle tepelsko-barrandienské jednotky, je převážně bez vulkanitů a jsou pro ni typické klastické sedimenty flyšového charakteru. Ve východní části tepelsko-barrandienské jednotky jsou tyto vulkanosedimentární sledy velmi málo metamorfovány (anchimetamorfovány). Kříbek et al. (2000) interpretovali geotektonický vývoj barrandienského proterozoika jako výsledek několika procesů: vzniku ostrovního oblouku, zaobloukového bazénu a zbytkového oblouku, inverze zaobloukové pánve a její polyfázovou deformaci, postorogenní extenze a denudace.

Stěžejním problémem pro interpretace kadomského geotektonického vývoje barrandienského neoproterozoika je kromě zjištění polarity neoproterozoického vulkanického oblouku odlišení kadomských a variských deformací v kadomském basementu. Tento problém lze dobře ilustrovat na příkladu regionální, tzv. jílovské kliváže, která porušuje neoproterozoické sedimenty v 80 km dlouhé zóně podél jv. okraje barrandienského proterozoika a byla dlouho považována za výsledek kadomské orogeneze, ačkoli v současné době byla reinterpretována jako struktura variského stáří (Rajlich et al., 1988; Žák et al., 2005a, b). Ve stejné oblasti byly nalezeny reliktní v.−z. struktury (vrásy) interpretované jako kadomské, zatímco struktury s dominantním směrem sv.−jz. byly považovány za variské. Podobně Zulauf et al. (1997) interpretoval barrovienskou metamorfní zonalitu a struktury v západní části tepelsko-barrandienské oblasti jako výsledek pozdně kadomského naklonění krustálních bloků směrem k východu, přetištěný kambro-ordovickým riftingem (transtenzí spojeným s fragmentací severního okraje Gondwany po kadomské orogenezi) a variskou kompresí sz.−jv. směru ve facii zelených břidlic, paralelní se směrem zkrácení varisky deformované pražské pánve vyplněné spodnopaleozoickými sedimenty (stáří střední kambrium až devon).

Je tedy zřejmé, že svrchní kůra tepelsko-barrandienské jednotky byla polyfázově

deformována jako výsledek kadomské orogeneze (což se projevuje v mapovém měřítku i cca 15° směrovou odchylkou předordovických a poordovických struktur či horninových pruhů), kambro-ordovického riftingu (transtenze) a variské orogeneze během svrchního devonu a spodního karbonu (Zulauf et al., 1997; Dallmeyer a Urban, 1998; Dörr et al., 2002). Kontroverzní interpretace a otázka kadomského vs. variského stáří deformačních struktur a metamorfózy tak provází geotektonické modely vývoje tepelsko-barrandienské jednotky za posledních sto let.

Unikátní oblast, kde lze jednoznačně odlišit tyto kadomské deformační události proterozoického basementu od kambro-ordovické transtenze a pozdějších variských procesů je sz. okraj pražské pánve (sz. křídlo barrandienského proterozoika) na území mezi Berounem a Rakovníkem. Stýkají se zde tři základní geologické jednotky: neoproterozoický basement, kambro-ordovické vulkanity křivoklátsko-rokycanského pásma a nadložní diskordantně uložené sedimenty spodního paleozoika. Tato oblast je rovněž výborně odkryta ve srovnání s jinými částmi tepelsko-barrandienské jednotky, zejména údolí řeky Berounky a jejích přítoků mezi Skryjemi a Berounem poskytuje téměř kontinuální několik desítek km dlouhý profil barrandienským proterozoikem, vulkanity křivoklátsko-rokycanského pásma a nadložními paleozoickými sedimenty pražské pánve. Hlavním cílem předkládané rigorózní práce bylo detailní srovnání finitních deformačních struktur v těchto třech jednotkách, což mělo pomoci jednoznačně vymezit tektonické události jednotlivých geotektonických cyklů a pomoci dešifrovat strukturní záznam kadomských tektonických procesů ve svrchní kůře perigondwanských teránů.

Literatura

Ballevre, M., Goff, E. L. & Hebert, R. 2001. The tectonothermal evolution of the Cadomian belt of northern Brittany, France: a Neoproterozoic volcanic arc. Tectonophysics 331, 19-43.

Dallmeyer, R. D. & Urban, M. 1998. Variscan vs Cadomian tectonothermal activity in northwestern sectors of the Teplá-Barrandian zone, Czech Republic: constraints from 40Ar/39Ar ages. Geologische Rundschau 87, 94-106.
Dorr, W., Zulauf, G., Fiala, J., Franke, W. & Vejnar, Z. 2002. Neoproterozoic to Early Cambrian history of an active plate margin in the Teplá–Barrandian unit - a correlation of U–Pb isotopic-dilution-TIMS ages (Bohemia, Czech Republic). Tectonophysics 352, 65-85.
Kříbek, B., Pouba, Z., Skoček, V., Waldhausrová, J. 2000. Neoproterozoic of the Teplá-Barrandian Unit as a part of the Cadomian orogenic belt: a review and correlation aspects. Bulletin of Geosciences 75, 175-194.
Murphy, J. B., Eguiluz, L. & Zulauf, G. 2002. Cadomian Orogens, peri-Gondwanan correlatives and Laurentia–Baltica connections. Tectonophysics 352, 1-9.
Murphy, J. B., Pisarevsky, S. A., Nance, R. D. & Keppie, J. D. 2004. Neoproterozoic-Early Paleozoic evolution of peri-Gondwanan terranes: implications for Laurentia-Gondwana connections. International Journal of Earth Sciences 93, 659-682.
Nance, R. D. & Murphy, J. B. 1994. Contrasting basement isotopic signatures and the palinspastic restoration of peripheral orogens: example from the Neoproterozoic Avalonian-Cadomian belt. Geology 22, 617-620.
Nance, R. D., Murphy, J. B. & Keppie, J. D. 2002. A Cordilleran model for the evolution of Avalonia. Tectonophysics 352, 11-31.
Rajlich, P., Schulmann, K. & Synek, J. 1988. Strain analysis on conglomerates from the Central Bohemian Shear Zone. Krystalinikum 19, 119-134.
Zulauf, G., Dorr, W., Fiala, J. & Vejnar, Z. 1997. Late Cadomian crustal tilting and Cambrian transtension in the Tepla-Barrandian unit (Bohemian Massif, Central European Variscides). Geologische Rundschau 86, 571-584.
Žák, J., Holub, F. V. & Verner, K. 2005a. Tectonic evolution of a continental magmatic arc from transpression in the upper crust to exhumation of mid-crustal orogenic root recorded by episodically emplaced plutons: the Central Bohemian Plutonic Complex (Bohemian Massif). International Journal of Earth Sciences 94(3), 385-400.
Žák, J., Schulmann, K. & Hrouda, F. 2005b. Multiple magmatic fabrics in the Sázava pluton (Bohemian Massif, Czech Republic): a result of superposition of wrench-dominated regional transpression on final emplacement. Journal of Structural Geology 27(5), 805-822.

Podrobný seznam použité literatury je rovněž součástí přiložené publikace (část 4).

4. Hlavní část − publikace

Hajná, J., Žák, J., Kachlík, V., Chadima, M. 2010. Subduction-driven shortening and differential exhumation in a Cadomian accretionary wedge: the Teplá–Barrandian unit, Bohemian Massif. *Precambrian Research* **176**, 27−45.

Precambrian Research 176 (2010) 27–45

Contents lists available at ScienceDirect

Precambrian Research

journal homepage: www.elsevier.com/locate/precamres

Subduction-driven shortening and differential exhumation in a Cadomian accretionary wedge: The Teplá–Barrandian unit, Bohemian Massif

Jaroslava Hajná[a,*], Jiří Žák[a,b], Václav Kachlík[a], Martin Chadima[c,d]

[a] Institute of Geology and Paleontology, Faculty of Science, Charles University, Albertov 6, Prague, 12843, Czech Republic
[b] Czech Geological Survey, Klárov 3, Prague, 11821, Czech Republic
[c] AGICO Inc., Ječná 29, Brno, 62100, Czech Republic
[d] Institute of Geology, Academy of Sciences of the Czech Republic, v.v.i., Rozvojová 269, Prague, 16500, Czech Republic

ARTICLE INFO

Article history:
Received 19 May 2009
Received in revised form 12 October 2009
Accepted 24 October 2009

Keywords:
Accretionary wedge
Anisotropy of magnetic susceptibility (AMS)
Bohemian Massif
Cadomian orogeny
Teplá–Barrandian unit
Variscan orogeny

ABSTRACT

The Teplá–Barrandian unit (TBU) of Central Europe's Bohemian Massif exposes perhaps the best preserved fragment of an accretionary wedge in the Avalonian–Cadomian belt, which developed along the northern active margin of Gondwana during Late Neoproterozoic. In the central TBU, three NE–SW-trending lithotectonic units (Domains 1–3) separated by antithetic brittle faults differ in lithology, style and intensity of deformation, magnetic fabric (AMS), and degree of Cadomian regional metamorphism. The flysch-like Domain 1 to the NW is the most outboard (trenchward) unit which has never been significantly buried and experienced only weak deformation and folding. The central, mélange-like Domain 2 is characterized by heterogenous intense deformation developed under lower greenschist facies conditions, and was thrust NW over Domain 1 along a SE-dipping fault. To the SE, the most inboard (arcward) Domain 3 is lithologically monotonous (dominated by graywackes and slates), was buried to depths corresponding up to the lower greenschist facies conditions, where it was overprinted by a pervasive SE-dipping cleavage and then was exhumed along a major NW-dipping normal fault.

We interpret these domains to represent allochtonous tectonic slices that were differentially buried and then exhumed from various depths within the accretionary wedge during Cadomian subduction. The NW-directed thrusting of Domain 2 over Domain 1 may have been caused by accretion at the wedge front, whereas the SE-dipping cleavage and SE-side-up exhumation of Domain 3 may record inclined pervasive shortening during tectonic underplating and subsequent horizontal extension of the rear of the wedge. The boundary faults were later reactivated during Cambro–Ordovician extension and Variscan compression.

Compared to related terranes of the Cadomian belt, the TBU lacks exposed continental basement, evidence for regional strike-slip shearing, and extensive backarc magmatism and LP–HT metamorphism, which could be interpreted to reflect flat-slab Cadomian subduction. This, in turn, suggests that Cadomian accretionary wedges developed in a manner identical to those of modern settings, elevating the TBU to a key position for understanding the style, kinematics, and timing of accretionary processes along the Avalonian–Cadomian belt.

1. Introduction

The Avalonian–Cadomian belt developed as a collage of microcontinents, accretionary complexes, island arcs, and intervening sedimentary basins along the northern active margin of Gondwana during Late Neoproterozoic (Nance et al., 1991; Nance and Murphy, 1994; Wortman et al., 2000; Murphy et al., 2002, 2004, 2006; Linnemann and Romer, 2002; von Raumer et al., 2002; Linnemann et al., 2007, 2008a,b). Fragments of this once continuous belt are now found as tectonostratigraphic terranes dispersed within younger Appalachian, Caledonian, Variscan, and Alpine orogens (Fig. 1a and b; e.g., von Raumer et al., 2003). As a consequence of their involvement in younger orogens, the direct structural record of Cadomian tectonic processes in these terranes is commonly obscured leaving uncertainities as to the deformation style, kinematics, or even polarity of subduction (e.g., Kříbek et al., 2000; Drost et al., 2004; Sláma et al., 2008).

An excellent setting where the Cadomian basement is superbly exposed and where the Cadomian structures can be examined in detail and unequivocally separated from Variscan (Late Devonian to Early Carboniferous) overprint is the Teplá–Barrandian unit (TBU) of the Bohemian Massif in Central Europe (Fig. 1). This

* Corresponding author. Fax: +420 221951452.
E-mail address: jaruska@cbcnet.cz (J. Hajná).

0301-9268/$ – see front matter © 2009 Elsevier B.V. All rights reserved.
doi:10.1016/j.precamres.2009.10.009

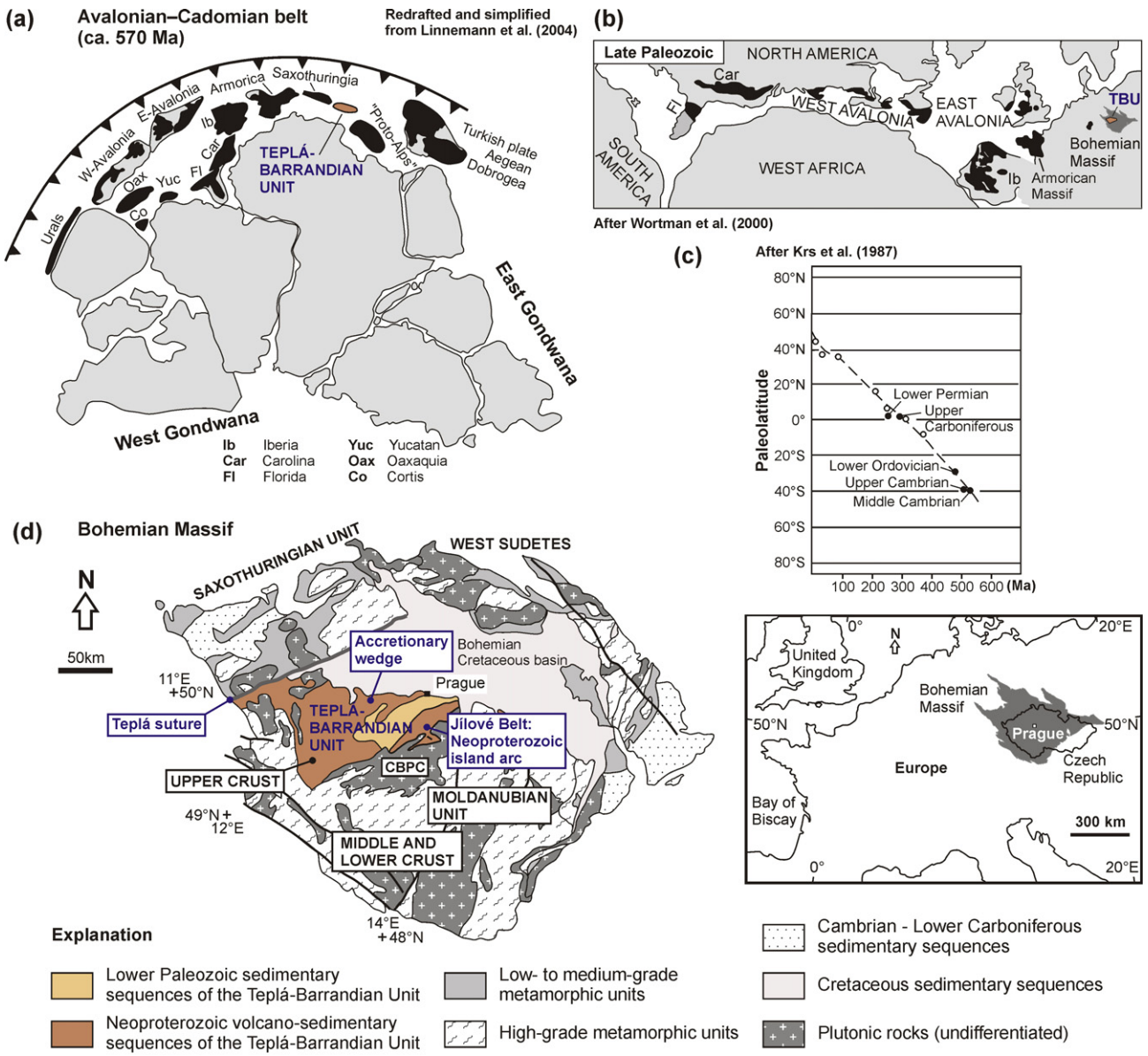

Fig. 1. (a) Paleogeographic position of the Teplá–Barrandian unit (TBU) within the Avalonian–Cadomian belt on the active northern margin of Gondwana during the Late Neoproterozoic (after Linnemann et al., 2004). (b) Paleogeographic reconstruction of the Avalonian–Cadomian terranes incorporated in younger orogens during Late Paleozoic (Wortman et al., 2000). (c) Paleozoic drift of the TBU estimated from paleomagnetic data (Krs et al., 1987). (d) Present-day position of the TBU in the central part of the Bohemian Massif. The TBU is interpreted to represent a Cadomian accretionary wedge between a paleo-subduction zone to the NW (Teplá suture) and an island arc (Jílové Belt) to the SE. Inset shows location of the Bohemian Massif in central Europe.

upper-crustal unit represents one of the easterly terranes of the Avalonian–Cadomian belt (Fig. 1a) and its central part has recently been interpreted to represent a fragment of Cadomian accretionary wedge (Dörr et al., 2002; Sláma et al., 2008) located between a paleo-subduction zone to the ~NW (present-day coordinates) and a volcanic arc to the ~SE (the Jílové Belt in Fig. 1d; see also detailed discussion and Fig. 12 in Sláma et al., 2008). This polarity of subduction is supported by the following evidence: (1) a Cadomian ~540 Ma ophiolite complex was accreted to the northwestern margin of the TBU before ~500 Ma (MLC in Fig. 2; Štědrá et al., 2002; Timmermann et al., 2004), (2) the proportion of detritic material derived from more evolved continental crust increases significantly to the SE (towards a retroarc basin southeast of the Jílové Belt volcanic arc; Sláma et al., 2008), and (3) complex deformation patterns, juxtaposition of contrasting lithotectonic units, and the presence of "block-in-matrix" mélanges (described in this paper) are typical of an accretionary wedge setting (e.g., Osozawa et al., 2009; Braid et al., in press).

In short, the protracted tectonic history of the TBU commenced with subduction, accretion, and island arc formation on the northern margin of Gondwana at ~660–560 Ma (e.g., Zulauf, 1997; Zulauf et al., 1997, 1999; Cháb, 1993; Kříbek et al., 2000; Dörr et al., 2002; Drost et al., 2004, 2007; Sláma et al., 2008), followed by arc/continent collision and deposition of sedimentary flysch successions at ~560–530 Ma (Sláma et al., 2008). Convergence changed to dextral transtension (Zulauf et al., 1997; Dörr et al., 2002; Linnemann et al., 2007, 2008b) during the Middle Cambrian to Early Ordovician, as portions of the Avalonian–Cadomian belt began to break-up and separate from the Gondwana margin (Linnemann et al., 2004, 2007; von Raumer and Stampfli, 2008). This process was associated with lithospheric thinning, extensive intra-plate magmatism, and deposition of Ordovician passive-margin successions

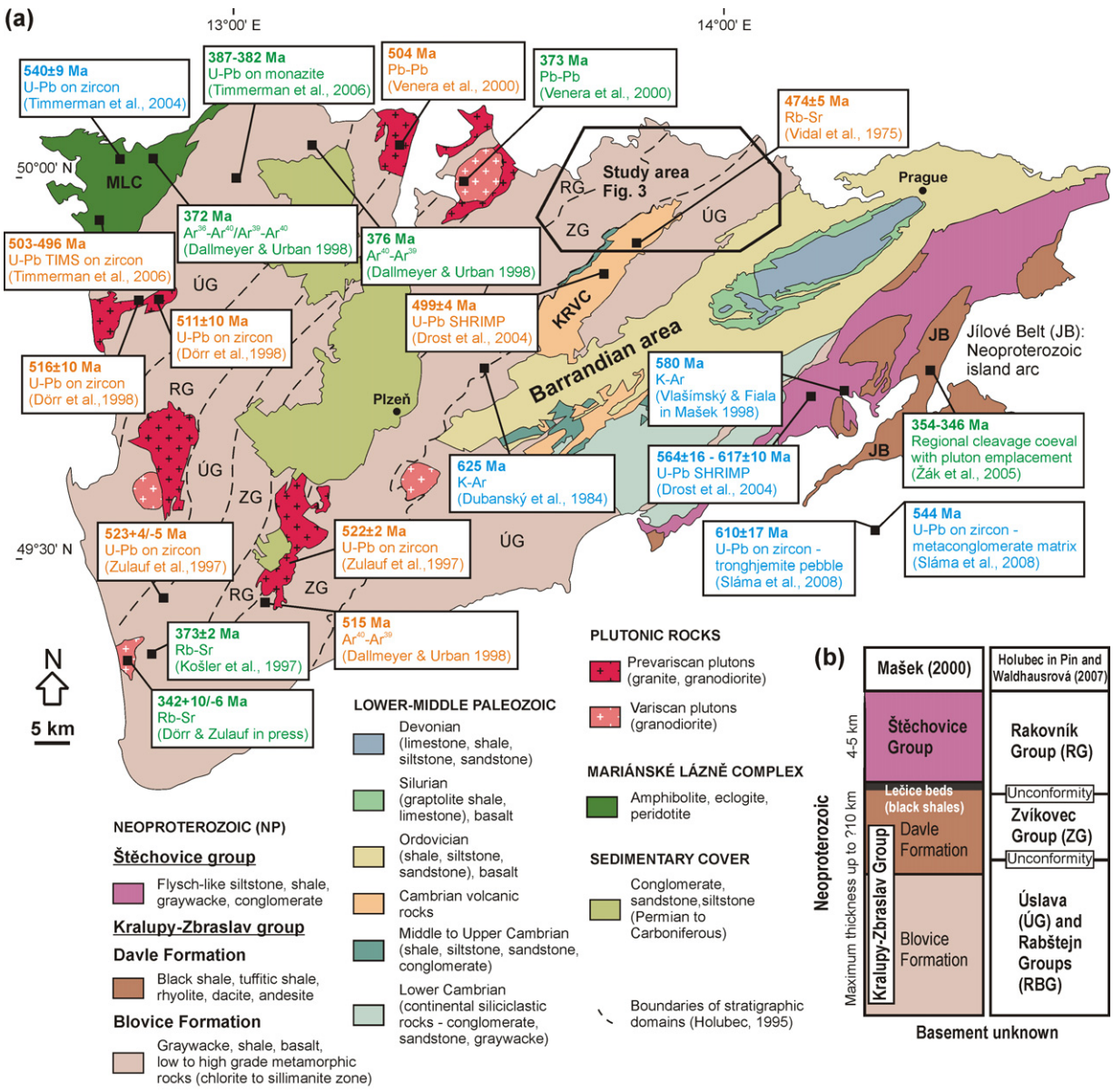

Fig. 2. (a) Simplified geologic map of the Teplá–Barrandian unit with selected geochronologic data (Cadomian, Cambro–Ordovician, and Variscan ages are distinguished by different colors). Redrafted from Geologic map of the Czech Republic, scale 1:500,000, published by the Czech Geological Survey in 2007. Lithologic units in the legend are arranged in stratigraphic order following Mašek (2000), dashed lines in the map correspond to lithostratigraphic belts of J. Holubec (cited in Pin and Waldhausrová, 2007). KRVC: Křivoklát–Rokycany volcanic complex, JB: Jílové Belt, MLC: Mariánské Lázně complex. (b) Comparison of two main lithostratigraphic concepts proposed for the Barrandian Neoproterozoic.

(Zulauf et al., 1997; Dörr et al., 1998; Kachlík and Patočka, 1998; Dostal et al., 2001; Pin et al., 2007). After the break-up and formation of the Rheic Ocean, the TBU drifted northward during the Early Paleozoic (Fig. 1c; Krs et al., 1987, 2001; Cocks and Torsvik, 2002; Patočka et al., 2003; Torsvik and Cocks, 2004) and was incorporated into the Variscan orogen during the Late Devonian to Early Carboniferous (Fig. 1b).

This paper describes in detail the geology, structure, magnetic fabric, and deformational microstructures of the Neoproterozoic basement in the central part of the TBU, just northwest of the Lower Paleozoic overlap sedimentary successions (referred to as "the Barrandian area"; Fig. 2a). On the basis of comparison of structures in the Neoproterozoic and Lower Paleozoic, we rigorously characterize and separate Cadomian deformation from subsequent Cambro–Ordovician transtension and Variscan shortening and propose a new kinematic model for the Teplá–Barrandian accretionary wedge during the Cadomian orogeny. Finally, we discuss plate-kinematic scenarios proposed for the TBU in comparison with those of the related Cadomian terranes (Saxothuringia, Armorica s.s.; Fig. 1a).

2. Geologic overview of the central part of the Teplá–Barrandian unit

The TBU is an upper-crustal block in the center of the Bohemian Massif, occupying the hanging-wall position with respect to the neighboring Saxothuringian and Moldanubian units (Figs. 1d and 2a; for review see, e.g., Vrána and Štědrá, 1997; McCann, 2008). The central part of the TBU consisting of low-grade Neoproterozoic to Lower Paleozoic volcanic and sedimentary rocks has never been buried to great depths, and escaped the Variscan (Late Devonian to Early Carboniferous) pervasive metamorphism and deformation.

2.1. Barrandian Neoproterozoic

The Neoproterozoic rocks of the TBU comprise volcano-sedimentary complex (the Kralupy–Zbraslav Group) conformably overlain by a flysch succession of the Štěchovice Group (Dallmeyer and Urban, 1998; Dörr and Zulauf, in press; Dubanský, 1984; Košler et al., 1997; Timmermann et al., 2006; Venera et al., 2000; Fig. 2b). For the sake of simplicity, we here use this widely adopted subdivision of Mašek (2000), however, in a companion paper we outline some new ideas on the TBU stratigraphy. In total, the thickness of both groups may exceed 10 km (a rough estimate by Chaloupský et al., 1995; Chlupáč et al., 1998); the real thickness is difficult to constrain due to unexposed basement, strong Cadomian and Variscan shortening, and crustal tilting.

The Kralupy–Zbraslav Group is composed of volcanic, volcaniclastic, and clastic sedimentary rocks and is further subdivided into the presumably older Blovice and younger Davle Formations (Mašek, 2000), which differ in their spatial distribution (Fig. 2) and in the composition of volcanic rocks. Two compositional groups of basalts have been defined in the Blovice Formation. One group is similar to recent MORB and E-MORB and indicates formation from REE-depleted mantle sources in a suprasubduction zone environment (Pin and Waldhausrová, 2007). The other, probably younger group of basalts is transitional and more evolved (similarly to recent OIB), lacks features of suprasubduction mantle metasomatism, and was presumably derived from a REE-enriched mantle source (Pin and Waldhausrová, 2007). In contrast, calc-alkaline basalts, andesites, dacites, rhyolites, and associated volcaniclastic rocks are typical of the Davle Formation (exposed in antiformal structures along the SE flank of the TBU; Fig. 2), including the Jílové Belt which may represent a fringing volcanic arc system (Fig. 1d; Waldhausrová, 1984) developed on oceanic crust close to the continental margin (see Sláma et al., 2008 for details).

The clastic sedimentary rocks of the Kralupy–Zbraslav Group include rhythmically interbedded shales and siltstones alternating with graywackes, the former indicating sedimentation in a deep-water, less dynamic environment, while the latter has been interpreted as turbidite and gravity-flow sediments (Cháb and Pelc, 1968; Dörr et al., 2002). Slump structures and olistoliths are locally abundant in 10–100 m-wide zones within the graywacke–shale sequences. The graywackes contain significant amounts of island-arc-derived material (Jakeš et al., 1979; Lang, 2000); the contribution from the mainland continental crust is minor in the Blovice Formation but increases to the SE (in the overlying Štěchovice Group; Sláma et al., 2008). In addition, the clastic sedimentary rocks of the Blovice Formation locally contain 10–100 m-thick lenses of chert of diverse origin (Pouba and Kříbek, 1986; Fatka and Gabriel, 1991; Pouba et al., 2000) and rare limestone intercalations.

The uppermost part of the Kralupy–Zbraslav Group is capped by up to 150 m-thick horizon of silicified black shales (the Lečice beds), passing upwards into flysch-like, rythmically alternating shales, siltstones, graywackes, and polymictic conglomerates of the Štěchovice Group. Syn-sedimentary textures (e.g., graded bedding, slump structures, flute marks) and inferred depositional processes (various types of turbidites, debris flows and mudflows) are indicative of relatively deep-water flysch-like sedimentation. Volcanic rocks are absent except for thin tuff and tuffite beds and ~540–520 Ma boninite dikes (Dörr et al., 2002; Sláma et al., 2008).

2.2. Barrandian Lower Paleozoic

The Neoproterozoic basement is unconformably overlain by unmetamorphosed Lower Cambrian to Middle Devonian sedimentary successions and associated volcanic complexes (e.g., Chlupáč et al., 1998; Štorch, 2006). In brief, the Lower Paleozoic rocks comprise (1) Lower Cambrian molasse-type continental siliciclastic deposits interpreted to have formed in intramontane basins within the Cadomian orogen (Patočka and Štorch, 2004), passing upwards into Middle Cambrian marine shales (overview in Geyer et al., 2008), (2) an Upper Cambrian to Lower Ordovician subaeric calc-alkaline volcanic suite ranging from minor basalts to andesites, dacites, and widespread rhyolites (Vidal et al., 1975; Waldhausrová, 1971; Pin et al., 2007), (3) a >2 km-thick sequence of Ordovician passive-margin siliciclastic and associated submarine within-plate rift-related basic volcanic rocks, (4) Silurian graptolite shales, basic volcanic and pyroclastic rocks, and limestone/shale interbeds in the upper part of the succession, and (5) Lower Devonian limestones and subordinate shales passing upward into Middle Devonian (Givetian) flysch-like siltstones and sandstones, the latter indicating the onset of the Variscan orogeny.

2.3. Existing geochronology

Radiometric ages from the TBU fall into three main groups (Fig. 2a and references therein), reflecting the major episodes in its tectonic history: (1) the Cadomian orogeny from ~620 to 560 (a period of island arc growth and active subduction) to ~530 Ma (flysch sedimentation and deformation of arc-derived siliciclastic rocks; Sláma et al., 2008); (2) a period of extensive magmatism at the end of Cambrian to the early Ordovician (~524–474 Ma) associated with intracontinental rifting during the break-up of the northern margin of Gondwana (Pin et al., 2007); and (3) Late Devonian (~382 and ~371 Ma) and early Carboniferous (~354–343 Ma) Variscan overprinting deformation and plutonism, localized particularly along margins of the TBU (Fig. 2a).

3. Geology of the northwestern margin of the Barrandian area

From NW to SE, the following key geologic units make up the northwestern margin of the Barrandian area (Fig. 3):

(1) The Barrandian Neoproterozoic consists here of three lithologically distinct ~NE–SW-trending belts. The northwestern belt (Figs. 3 and 4a; the Kralovice–Rakovník belt of Röhlich, 1965; or flysch facies of Cháb and Pelc, 1968) is a very-low-grade flysch-like sequence of rhythmicaly alternating graywackes, slates, and siltstones devoid of volcanic rocks. The average thickness of graywacke beds ranges from 20 cm to several meters, the thickness of slate interbeds varies from several centimeters to decimeters. The central belt (Figs. 3 and 4b and c; the Radnice–Kralupy belt of Röhlich, 1965 or volcanogenic facies of Cháb and Pelc, 1968) is more complex, consisting of graywackes, slates, and siltstones with abundant syn-sedimentary slump structures and olistoliths (Cháb and Pelc, 1968; Mašek, 2000), and up to km-scale lens-shaped to irregular bodies of tholeiitic (MORB-like and P-MORB) to alkaline basalts (Fiala, 1977; Pin and Waldhausrová, 2007). This mélange-like unit contains structurally isolated graywacke blocks and fragments of ocean floor (both up to several hundreds meters in size) dispersed in host slates and presumably represents a broken formation (Hsü, 1968; or graywacke-argillite mélange of Cowan, 1974). By contrast, the southeasterly Zbiroh–Šárka belt (Figs. 3 and 4d; Röhlich, 1965; monotonous facies of Cháb and Pelc, 1968) is dominated by graywackes, siltstones and slates (Fig. 4d) with abundant lenses of chert.

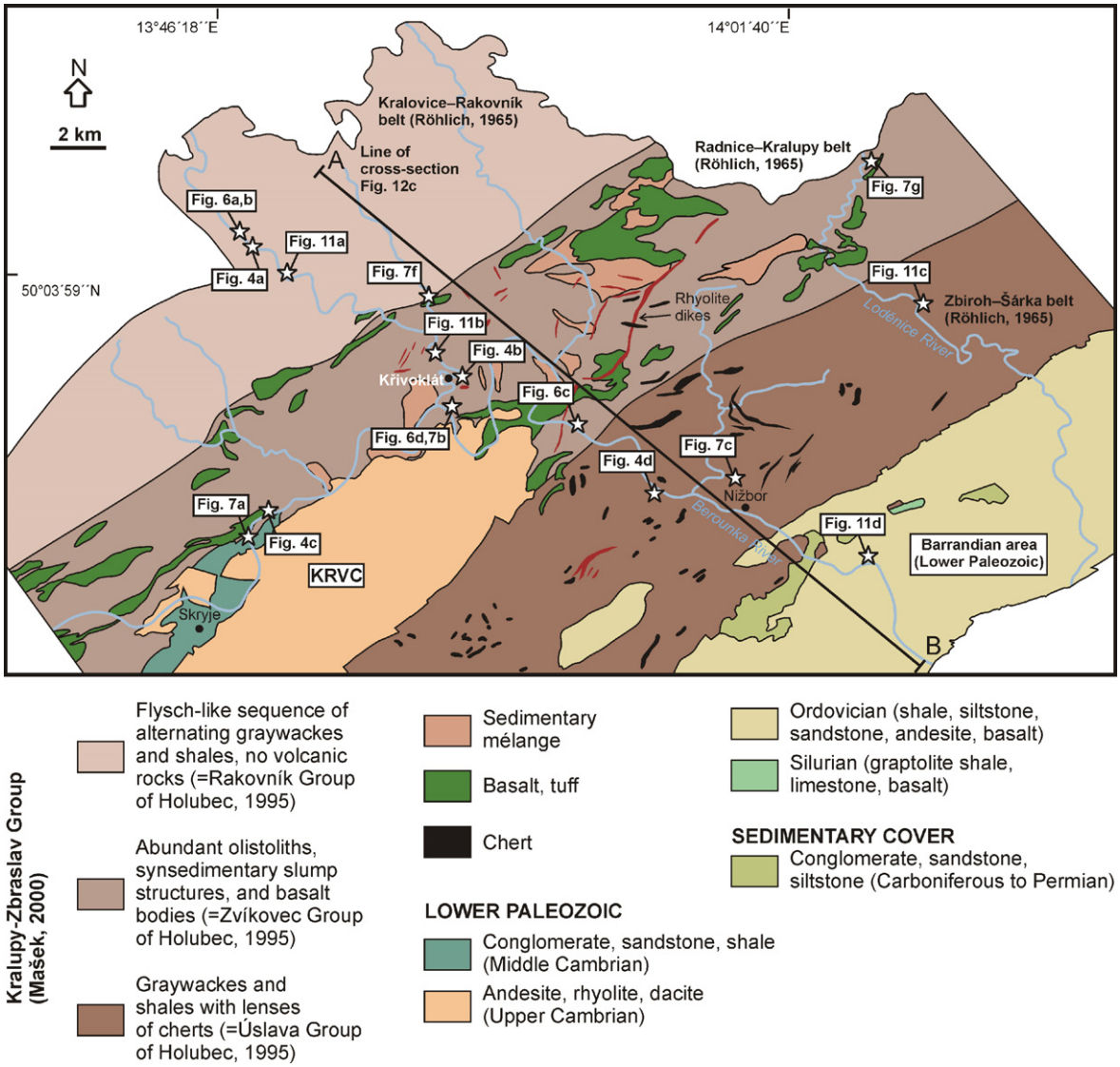

Fig. 3. Simplified geologic map of the study area along the northwestern margin of the Barrandian Lower Paleozoic. Geology and lithostratigraphic belts compiled from Geologic map of the Křivoklát area 1:50,000 published by the Czech Geological Survey in 1997, and geologic map of the Czech Republic 1:50,000 sheets 12–41 Beroun and 12–23 Kladno. Stars indicate location of photographs, line A–B shows location of cross-section (see Fig. 12c).

(2) In the south-central part of the area, unmetamorphosed Middle Cambrian marine conglomerates, sandstones, and shales (~200 m total thickness) unconformably overlie the Neoproterozoic basement rocks (Fig. 3). This spectacular angular unconformity was first described by Kettner (1923) and Kettner and Slavík (1929).

Both the Neoproterozoic and Middle Cambrian strata are capped by the Upper Cambrian to Lower Ordovician Křivoklát–Rokycany volcanic complex (KRVC in Fig. 3; Waldhausrová, 1966, 1971; Vidal et al., 1975; Pin et al., 2007), a ~NE–SW-trending belt up to 1500 m thick, consisting of multiple stacked subaerial lava flows of basaltic to rhyolitic composition, and subordinate explosive volcanic products (ignimbrites, coarse-grained agglomerates). To the N and NW of the complex, rhyolite dikes of unknown radiometric age cut across the host Neoproterozoic rocks. In spite of some differences in geochemistry and textures, the dikes closely resemble felsic rocks of the uppermost part of volcanic complex.

(3) To the southeast, Lower Paleozoic (Ordovician and Silurian) sedimentary rocks of the Prague Basin (Chlupáč et al., 1998) regionally overlap the Neoproterozoic basement (Fig. 3). The basal Ordovician marine shallow-water conglomerates, sandstones, and graywackes contain clasts of Neoproterozoic chert and Upper Cambrian volcanic rocks. Younger formations comprise Lower to Middle Ordovician quartzites, shales and sandstones, accompanied by a thick complex of predominantly basic submarine lavas and volcaniclastic rocks (Chlupáč et al., 1998). Silurian rocks are represented by black graptolite shales, carbonatic shales, and limestones.

4. Structural pattern

In the Neoproterozoic rocks along the northwestern margin of the Barrandian area, we define three contrasting ~NE–SW-trending structural domains (Fig. 5) on the basis of their lithology, mesoscopic structures, magnetic fabric, microstructural characteristics, and mineral associations as described below. These structural domains roughly correspond to the lithostratigraphic belts defined previously at much larger-scale by Röhlich (1965), Cháb and Pelc (1968), or in an unpublished report by J. Holubec (cited

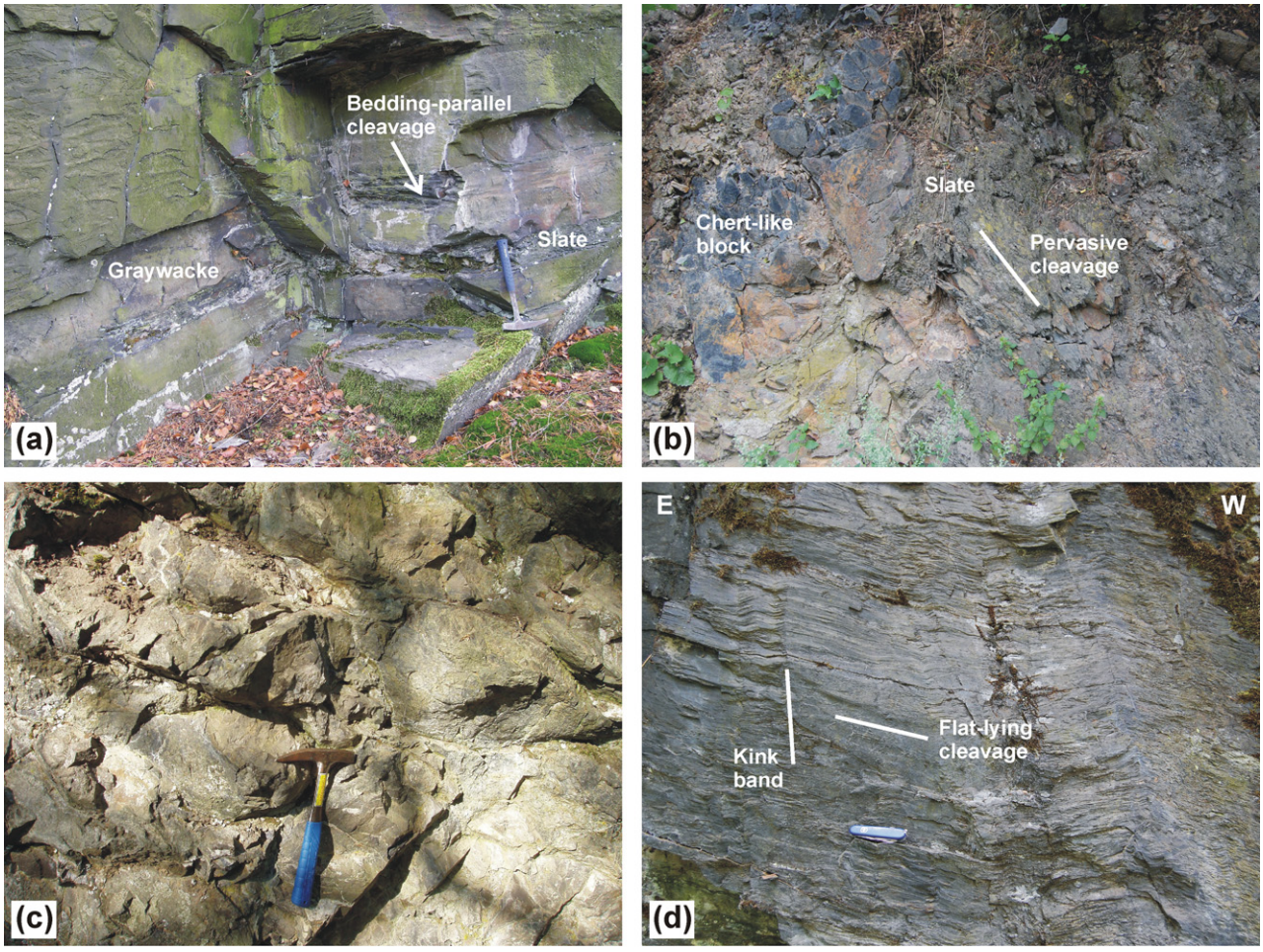

Fig. 4. Characteristic lithologic features of the Neoproterozoic rocks along the northwestern margin of the Barrandian area. (a) Bedding in alternating graywackes and slates typical of Domain 1. Cleavage is localized in incompetent thin slate interbeds; Dolní Chlum. Hammer for scale. (b) Chert-like block (olistolith?) in pervasively deformed slate, Domain 2; Křivoklát. Block width is 20 cm. (c) Deformed pillow lava, Domain 2; Čertova skála. Hammer for scale. (d) Pervasive cleavage in slates, Domain 3; Žloukovice. Swiss Army penknife (9 cm long) for scale. See Fig. 3 for location of outcrops.

in Pin and Waldhausrová, 2007; Fig. 3). In this study, we use descriptive terms ("Domains 1–3"—numbered consecutively from the NW to the SE; Fig. 5) to avoid any stratigraphic implications.

4.1. Domain 1

Well-defined bedding typical of Domain 1 (thick graywacke beds with thin slate interbeds; Fig. 4a) either strikes ~ENE–WSW and dips gently (~10–30°) to the ~NNW (in the southwestern part of the area), or strikes ~NE–SW and dips gently to the ~NW (Fig. 5). Bedding-parallel cleavage is localized preferentially in the incompenent slate interbeds, while the more rigid graywackes are either entirely devoid of macroscopically discernible cleavage or contain only a locally developed weak spaced cleavage. A lineation, interpreted as slip lineation, is developed on cleavage planes in slates and is parallel to the stretching lineation in graywackes along contacts with slates. The lineation plunges gently (~10–25°) west, oblique to the strike of the bedding (Fig. 5).

Domain 1 is characterized by a simple fold style, expressed both on outcrop- and map-scale by the monoclinal orientation of the bedding. Significant localization of deformation into weak slates indicates that the dominant folding mechanism was flexural slip. Bedded sequences are locally cross-cut by meter-scale overthrusts and contractional duplexes (Fig. 6a and b).

4.2. Domain 2

Unlike Domain 1, well-defined bedding is preserved only in larger lenses or boudins of graywackes that are embedded in intensely deformed finer-grained slates and graywackes. Bedding strike scatters widely but ~E–W bedding, dipping moderately to steeply ~N–NW dominates and is generally parallel to cleavage in the surrounding slates (Fig. 6c). The slates are characterized by pervasive cleavage that transposes the original bedding or fine-scale lamination (Fig. 6c) and is associated with weak or no lineation. The cleavage exhibits two main orientations. The dominant cleavage strikes ~ENE–WSW to ~ESE–WNW and dips moderately to steeply to the ~NNW–NNE or ~SSW (cleavage poles cluster around the maximum principal eigenvector 194°/37°; Fig. 5). However, some cleavages are steep, dipping to the ~ENE or ~WSW (Fig. 5). In outcrop, the steep pervasive cleavage in the Neoproterozoic slates is unconformably overlain by only moderately tilted (50–60° to the ~SE) and unstrained Middle Cambrian basal sandstones and conglomerates (Fig. 7a).

To the N and NW of the Křivoklát–Rokycany volcanic complex, rhyolite dikes (Fig. 7b) and irregularly shaped rhyolite intrusions choked with abundant host rock xenoliths (magmatic breccias) cut across the pervasive cleavage in the Neoproterozoic slates along knife-sharp discordant contacts. The cleavage is also contained in the host rock xenoliths and rafts within the dikes.

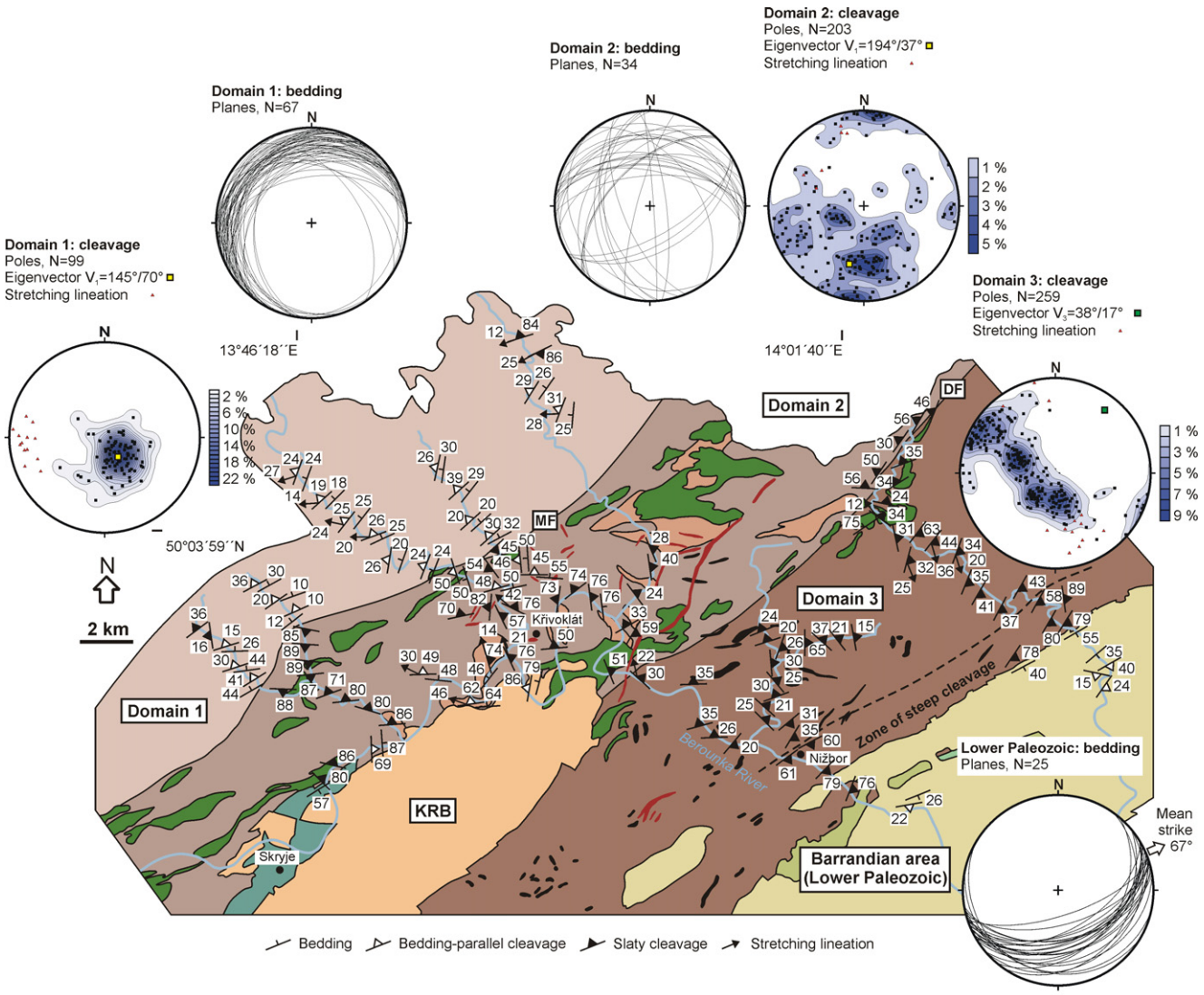

Fig. 5. Structural map of the study area showing contrasting structural patterns in Domains 1–3 and overlying Lower Paleozoic rocks. Stereonets (equal area projection, lower hemisphere) show orientation of bedding, cleavage, and stretching lineation. Lithologic units colored as in Fig. 3. DF: Družec fault, KRVC: Křivoklát–Rokycany volcanic complex, MF: Městečko fault.

Two distinct types of folds were documented in Domain 2 depending on lithology: rare meter-scale tight to isoclinal upright folds occur in competent graywacke beds, and tight chevron folds and contractional monoclinal kink-bands occur in slates, with their axial planes dipping steeply to the NW. While cleavage is axial-planar to the first type of folds, the kink-bands are superposed onto the pre-existing cleavage.

4.3. Domain 3 and Barrandian Lower Paleozoic overlap sequence

Graywackes and slates in Domain 3 are characterized by intensely developed pervasive cleavage with only rarely discernible bedding or lamination (Figs. 4d and 6d). On a stereonet, cleavage poles define a girdle around a subhorizontal ~NE–SW axis (mean calculated as the minimum eigenvector of the orientation tensor is 038°/17°). The cleavage shows bimodal orientation in much of the Domain, either striking ~NE–SW and dipping moderately to the ~SE, or striking ~NW–SE and dipping shallowly to moderately to the ~NNW–NE (Fig. 5). Within a 2 km-wide zone along the contact with the overlying Barrandian Lower Paleozoic rocks, the cleavage progressively steepens while maintaining the ~NE–SW strike and ~SE dip (Fig. 5).

As with Domain 2, the angular unconformity between the Neoproterozoic slates and overlying basal Ordovician beds is well-documented both in outcrop and at map-scale in the southeastern part of the area (Fig. 5). Here, cleavage in the Neoproterozoic slates dips steeply to the ~SE and is sharply truncated by the overlying basal Ordovician strata. Bedding in both the basal conglomerates and overlying younger formations strikes ~ENE–WSW and dips moderately to the ~SSE (mean strike is 067°). The Lower Paleozoic strata are devoid of cleavage, except for bedding-parallel cleavage in shale interbeds between competent sandstones.

Fold style in the Neoproterozoic slates is identical to that of Domain 2: meter-scale chevron folds (Fig. 7c) and contractional conjugate and monoclinal kink-bands are superposed on the pre-existing flat-lying and steep cleavage, respectively (Figs. 4d and 7d and e). Where the cleavage is steep along the contact with the Barrandian Lower Paleozoic (Fig. 5), the kink-band axial planes dip shallowly to moderately ~NW (Fig. 7e), whereas in flat-lying cleavage away from the contact zone they dip moderately to steeply ~NW and ~SE (Fig. 7d).

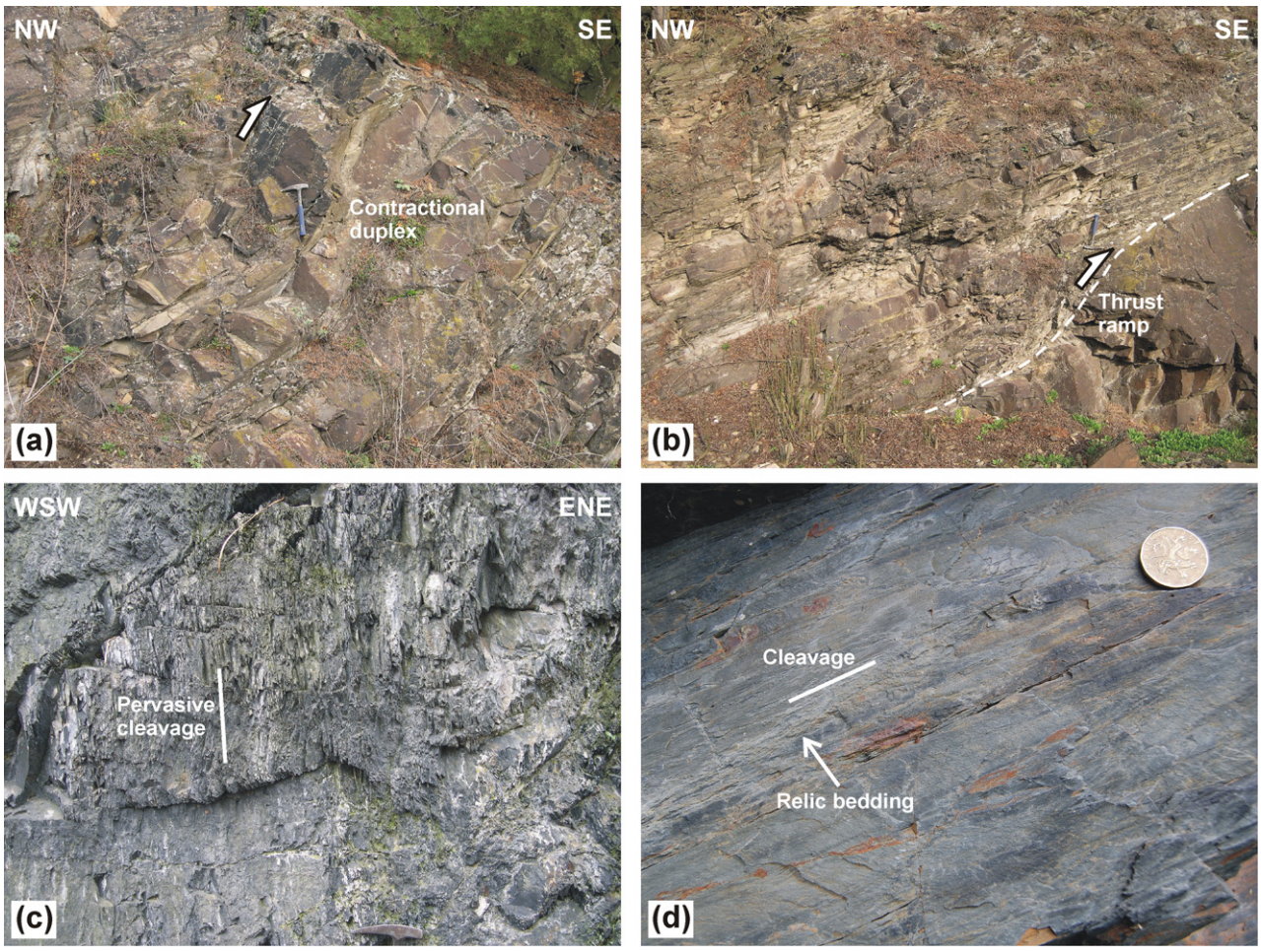

Fig. 6. Mesoscopic deformational structures in the Neoproterozoic rocks. (a and b) Contractional duplexes and thrust faults in rhytmically interbedded graywacke–slate sequences of Domain 1; Chlum u Rakovníka. Hammer for scale. (c) Steep pervasive cleavage in slates, Domain 2; Roztoky u Křivoklátu. Hammer for scale. (d) Relic bedding-parallel to intensely developed cleavage, Domain 3; Račice. Hammer for scale. See Fig. 3 for location of outcrops.

4.4. The nature of domain boundaries

At map-scale, the boundaries between structural domains are expressed as ~NE–SW-trending sharp structural breaks, truncating bedding and cleavage on either side. Structures and lithology are remarkably discordant across the domain boundaries (Fig. 5).

The boundary between Domains 1 and 2 (referred here to as the Městečko fault; MF in Fig. 5) was documented on one outcrop as a more than ~10 m wide zone of intensely deformed and mineralized fault breccia consisting of angular fragments of graywackes and slates set in a fine-grained crushed matrix. The fault zone strikes ~NE–SW and dips moderately (~45°) to the SE, i.e., beneath Domain 2 (Fig. 7f). This orientation measured on the outcrop thus corresponds well with the general orientation of the boundary in the map (Fig. 5). Kinematic indicators are rare in the breccia zone; a few asymmetric non-brecciated blocks indicate top-to-the-NW kinematics (Domain 2 over Domain 1; Fig. 7f). In other places the boundary is not exposed, but can be well constrained to within a few tens of metres in the field and mapped as a line separating neighboring outcrops assigned to Domains 1 and 2.

The boundary between Domains 2 and 3 (referred here to as the Družec fault; DF in Fig. 5) is best exposed in its NE segment. Here, the flat-lying (25–35° dip) cleavage typical of Domain 3 is deflected into the boundary-parallel, ~NE–SW strike and steepens up to 60° dip to the NW (i.e., beneath the Domain 2). The rotated cleavage grades into meters to first tens of meters wide cataclastic zone (fault breccia in Fig. 7g). Within the cataclastic zone, both the (rotated) cleavage and overprinting cataclastic foliation have the same orientation, striking ~NE–SW and moderately to steeply dipping to the NW. These structural relations indicate SE-side-up kinematics (Domain 2 down, Domain 3 up).

5. Anisotropy of magnetic susceptibility (AMS)

Magnetic fabric, as derived from anisotropy of magnetic susceptibility (AMS; for reviews and basic principles of the method see, e.g., Hrouda, 1982; Tarling and Hrouda, 1993) was used to corroborate the structural data and to describe the fabric parameters and fabric gradients across the three structural domains (Figs. 8–10).

5.1. Methodology

Anisotropy of magnetic susceptibility is mathematically described as a symmetric second rank tensor which can be visualized as an ellipsoid; its semi-axis lengths, $k_1 \geq k_2 \geq k_3$, are termed the principal susceptibilities and their orientations, K_1, K_2, K_3, are denoted as the principal directions. Such an ellipsoid defines a magnetic fabric where the maximum direction (K_1) is denoted as magnetic lineation and the plane perpendicular to the minimum direction (K_3) and containing the maximum and intermediate directions (K_1, K_2) is denoted as magnetic foliation.

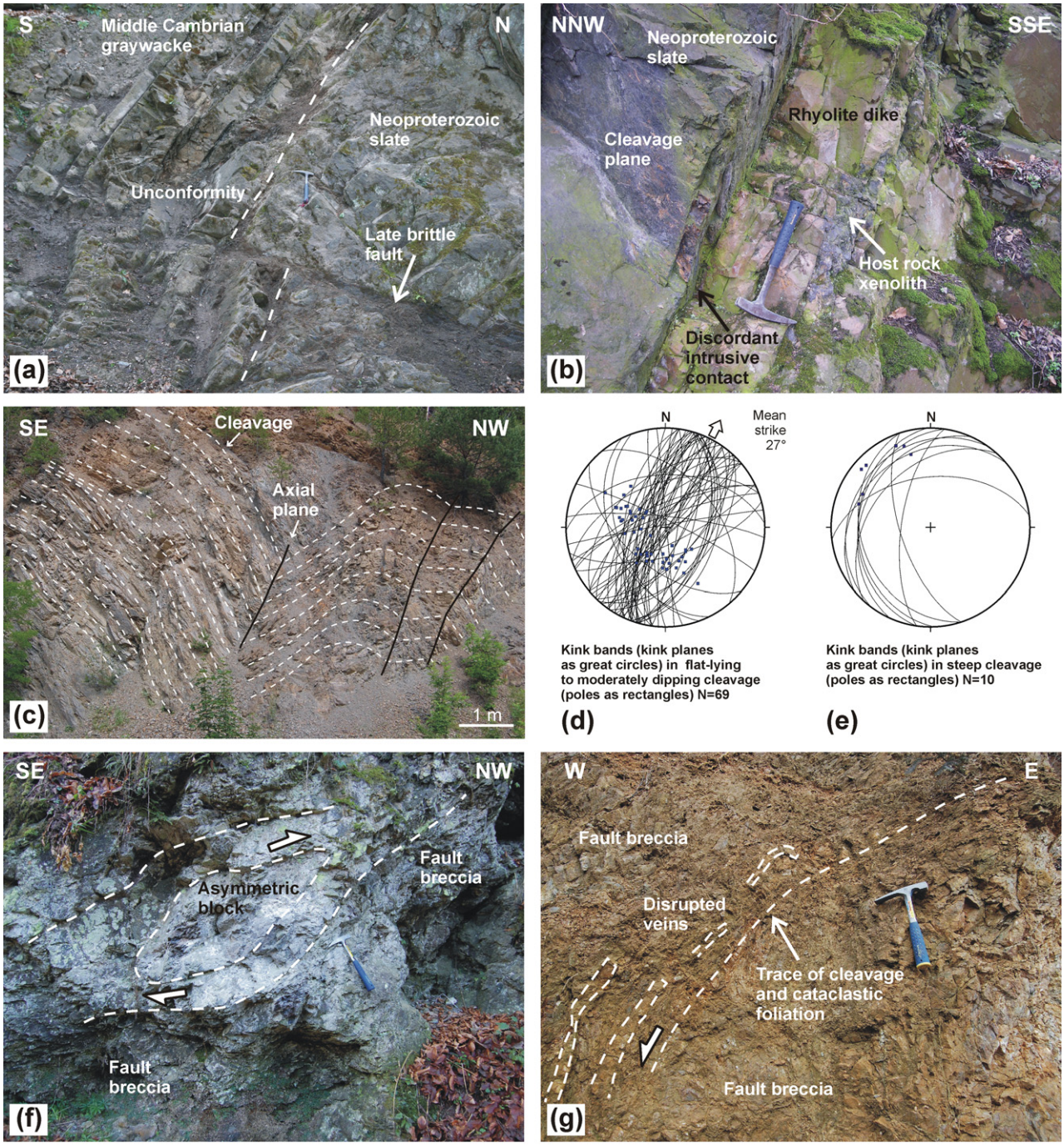

Fig. 7. (a) Angular uncomformity between the Neoproterozoic slates and Middle Cambrian graywackes, Domain 2; Týřovice. Hammer for scale. (b) Rhyolite dike cutting across steep cleavage in slates, Domain 2; Roztoky u Křivoklátu. Hammer for scale. (c) Chevron fold superposed on cleavage in slates, Domain 3; roadcut near Nižbor. (d and e) Stereonets (equal area projection, lower hemisphere) showing orientation of kink axial planes superposed on flat-lying and steep cleavage, Domain 3. (f) Cataclastic fault zone separating Domains 1 and 2 and showing top-to-the-NW kinematics; near Městečko. Hammer for scale. (g) Cataclastic fault zone separating Domains 2 and 3, rotated flat-lying cleavage indicates SE-side-up kinematics; Družec. Hammer for scale. See Fig. 3 for location of outcrops.

Quantitatively, AMS data can be described by bulk susceptibility, degree of anisotropy, and anisotropy shape parameter. Bulk (mean) susceptibility is calculated as an arithmetical mean of the principal susceptibilities, $k_b = (k_1 + k_2 + k_3)/3$, and reflects the type and relative content of magnetic minerals in a rock. Degree of anisotropy, expressed as $P = k_1/k_3$ (Nagata, 1961), reflects the intensity of magnetic fabric. Anisotropy shape parameter, calculated as $T = 2\ln(k_2/k_3)/\ln(k_1/k_3) - 1$ (Jelínek, 1981) quantitatively describes the shape of the anisotropy ellipsoid; it varies from −1 (perfectly prolate ellipsoid, i.e., linear fabric) through 0 (neutral or triaxial ellipsoid) to +1 (perfectly oblate ellipsoid, i.e., planar fabric).

In total, 66 oriented samples (cores 2.5 cm in diameter) were taken using a portable drill at 23 sampling sites in the Neoproterozoic rocks along two ~NW–SE oriented transects (Fig. 9). After laboratory cutting, these samples yielded 267 standard oriented specimens (ca. 2.2 cm in height). AMS measurements and other rock magnetic experiments were performed using an Agico MFK1-FA Multi-function Kappabridge coupled with a temperature control unit CS-3 at AGICO Inc., Brno, Czech Republic. Statistical analysis of

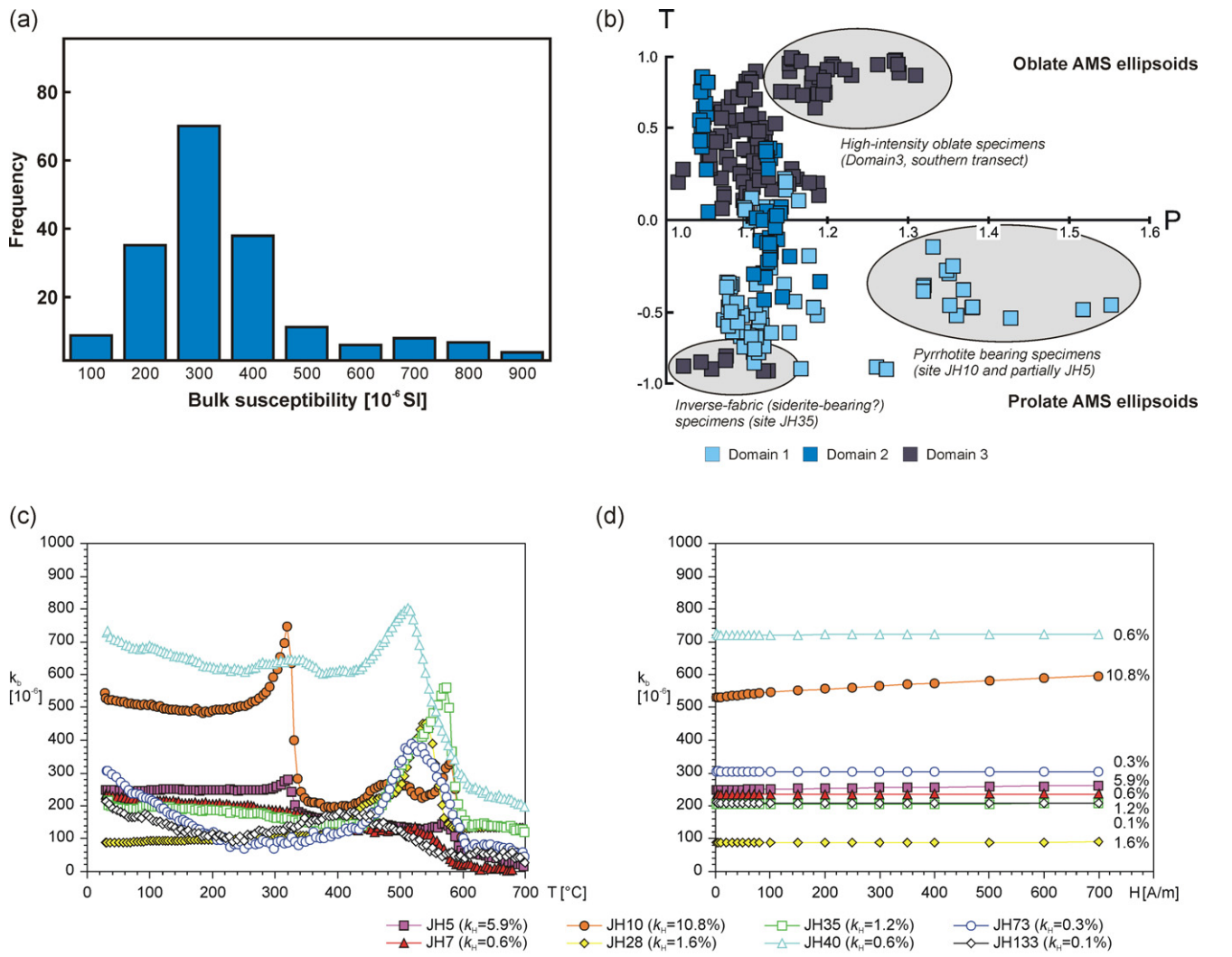

Fig. 8. (a) Histogram of bulk susceptibility and (b) the plot of the AMS intensity (P) vs. ellipsoid shape (T) of all analyzed specimens. (c) Magnetic susceptibility as a function of temperature, heating in air atmosphere, heating rate ca. 10 °C/min, and (d) magnetic susceptibility as a function of increasing AC field of eight representative samples. Field dependence is quantified as $k_H = 100 \times (k_{700} - k_{10})/k_{700}$, where k_x denotes a susceptibility measured in respective AC fields in A/m, peak values.

the AMS data was carried out using the ANISOFT 4.2 program (written by M. Chadima and V. Jelínek; www.agico.com). The calculated AMS parameters are listed in Electronic Supplementary Material.

5.2. Magnetic mineralogy

In all the investigated specimens bulk susceptibility does not exceed 1000×10^{-6} SI. The susceptibility distribution is slightly bimodal having one pronounced maximum at ca. 300×10^{-6} SI and the other indistinct maximum at ca. 700×10^{-6} SI (Fig. 8a). Relatively low susceptibility values indicate that the carriers of magnetic susceptibility are predominantly paramagnetic minerals, presumably phyllosilicates (in our case most probably chlorite and clastic biotite). Few specimens with relatively higher susceptibility values, however, may indicate the presence of another magnetic mineral.

For the majority of specimens the degree of magnetic anisotropy ranges from 1.03 to 1.20 with AMS ellipsoids being moderately prolate, neutral, to moderately oblate in shape (Fig. 8b). Such a distribution of magnetic fabric can be explained as being controlled by phyllosilicate grains with various types of preferred orientations provided that the magnetic anisotropy of a phyllosilicate grain is perfectly oblate having anisotropy degree $P \cong 1.30$ (Martín-Hernández and Hirt, 2003). In addition to the phyllosilicate-controlled fabric, some specimens display a high-intensity oblate fabric ($P \cong 1.15$–1.3, $T > 0.7$), a low-intensity highly prolate fabric ($P < 1.10$, $T < -0.8$), and a high-intensity moderately prolate fabric ($P \cong 1.30$–1.60, $T \cong -0.5$). Whereas the high-intensity oblate fabric can be carried by sub-parallel orientation of phyllosilicates, there is no means for obtaining such high-intensity or highly prolate fabrics solely by the preferred orientation of (oblate-anisotropy) phyllosilicate grains. These extreme cases of prolate fabric suggest that, at least in some specimens, the magnetic fabric is not exclusively dominated by the preferred orientation of paramagnetic phyllosilicates.

In order to analyze the carriers of magnetic fabric, magnetic susceptibility was measured as a function of temperature (from room temperature up to 700 °C, at a heating rate of ca. 10 °C/min) and amplitude of applied AC field (in the range of 2–700 A/m, peak values). For some analyzed specimens (Fig. 8c, JH10, JH40, JH73, JH133), magnetic susceptibility hyperbolically decreases as a function of increasing temperature up to ca. 300 °C, being more or less constant for the other specimens (JH5, JH7, JH28, JH35). Gradual hyperbolic decrease is typical behavior of paramagnetic minerals where magnetic susceptibility is inversely proportional to the absolute temperature. In some specimens (JH10 and JH5) there is a pronounced peak in susceptibility at ca. 320 °C corresponding to the Curie temperature of pyrrhotite. Further increase in susceptibility

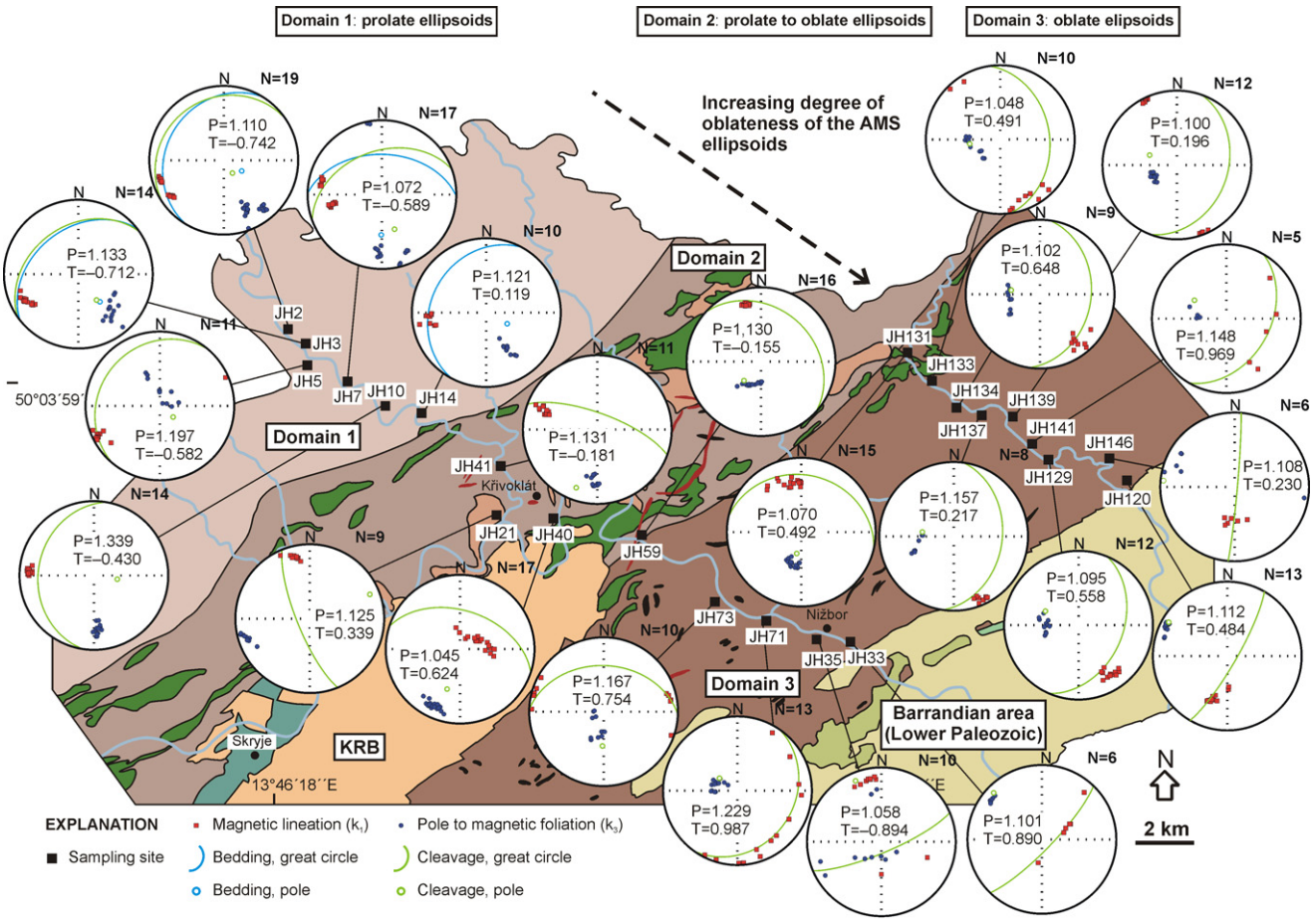

Fig. 9. Map of the northwestern margin of the Barrandian area showing AMS sample locations, mean *P* and *T* parameters at each sampling site, and orientation of magnetic lineations (k_1) and poles to magnetic foliations (k_3) in stereonets (equal area projection, lower hemisphere, geographic coordinate system).

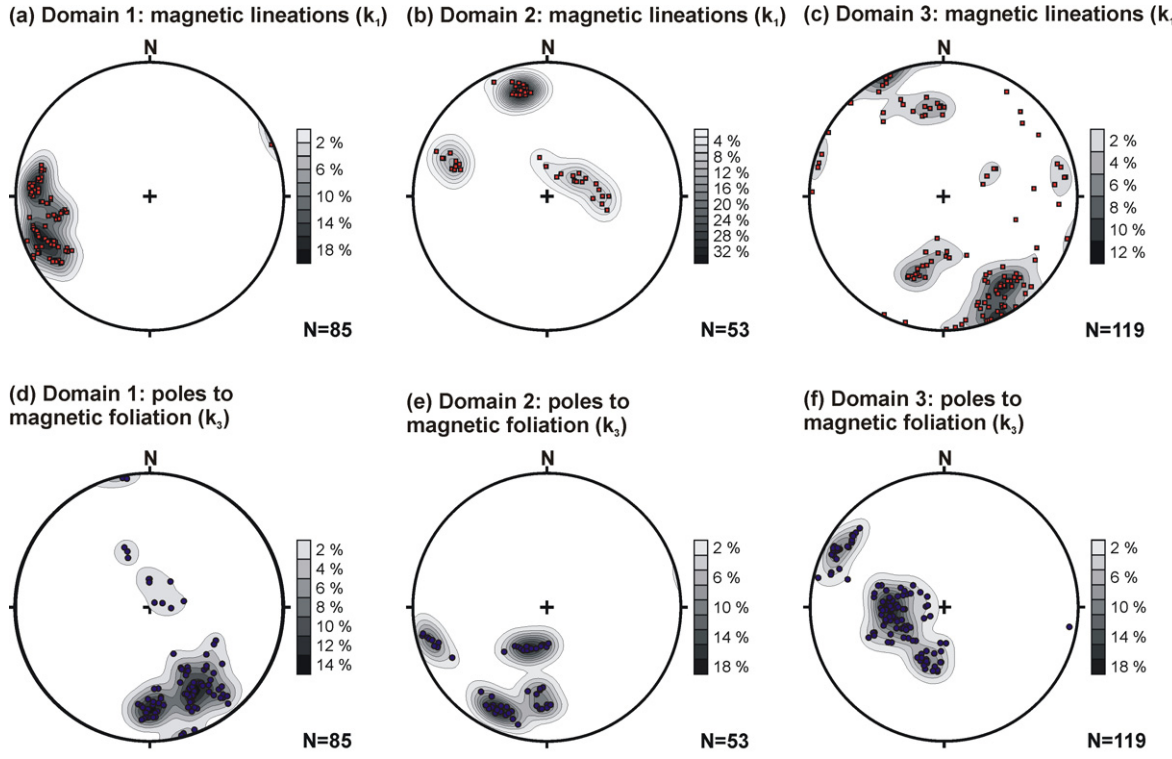

Fig. 10. Stereonets (equal area projection, lower hemisphere) summarizing orientation of magnetic lineations (k_1) and poles to magnetic foliations (k_3) for Domains 1–3.

above ca. 400 °C can be attributed to the growth of new magnetite as a result of phyllosilicate (and other iron minerals) decomposition and oxidation during increased temperature. Indeed, a sharp susceptibility decrease above ca. 550 °C corresponds to the Curie temperature of magnetite. The presence of pyrrhotite in some specimens (namely in JH10 and JH5) is further verified by increasing susceptibility as a function of applied field (Fig. 8d); field dependence starting at relatively low field is a characteristic feature of pyrrhotite (e.g., Worm et al., 1993). The field dependence of the other representative specimens is insignificant (Fig. 8d).

5.3. Magnetic fabric

Combining magnetic mineralogy analyses (Fig. 8c and d) and magnetic fabric data (Fig. 8a and b), the high-intensity, moderately prolate fabric cluster of specimens ($P \cong 1.30–1.60$, $T \cong -0.5$) is seen to correspond to sites JH10 and JH5 where the presence of pyrrhotite was demonstrated (Fig. 8c and d). The low-intensity highly prolate fabric ($P < 1.10$, $T < -0.8$) corresponds to site JH35, which exhibits an inverse magnetic fabric where both magnetic lineation and foliation are in inverse orientation with respect to the mesoscopic lineation and foliation (Fig. 9, JH35). Such a behavior in sedimentary rocks can be attributed to the magnetic fabric being controlled by siderite (e.g., Winkler et al., 1996; Chadima et al., 2006).

Since any regional fabric pattern can be studied only by comparing the magnetic fabrics in sites not significantly different in magnetic mineralogy, the pyrrhotite- and siderite (?)-bearing specimens are excluded from further interpretation. In their absence, a gradual spatial development of magnetic fabric can be observed going through the structural domains (Fig. 9). In Domain 1, the degree of anisotropy ranges from 1.07 to 1.20 with an average value of 1.16. The AMS ellipsoids are mostly prolate to neutral in shape ($T = -0.90–0.25$) (Figs. 8b and 9). The orientation of magnetic fabric is homogeneous—magnetic foliations strike ~NE–SW and dip moderately to steeply ~NW, whereas magnetic lineations plunge gently to the ~W–WSW (Figs. 9 and 10a and d).

In Domain 2, the degree of anisotropy is in the range 1.04–1.19. The shape parameter is between −0.48 and 0.88, so the AMS ellipsoids have neutral to oblate shapes (Figs. 8b and 9). Magnetic foliations exhibit four main orientations: (1) ~NNW–SSE dipping steeply ~ENE, (2) ~WNW–ESE dipping gently ~NNE, (3) ~WNW–ESE dipping steeply ~NNE, and (4) ~E–W dipping moderately to steeply ~N (Fig. 9). These orientations correspond to four distinct maxima of k_3 axes on the stereonet (Fig. 10e) and can be correlated with the rather scattered distribution of cleavage in Domain 2 (Fig. 5). Magnetic lineations cluster in three maxima plunging gently ~WSW, steeply ~NE, and gently ~NNW (Figs. 9 and 10b).

In Domain 3, the degree of anisotropy is in the range of 1.04–1.31. The shape parameter ranges between 0.10 and 0.99, which means that the AMS ellipsoids have only oblate shapes (Fig. 8b). On the stereonet, magnetic foliations cluster around two maxima, one corresponding to cleavage striking ~NW–SE to ~N–S and dipping gently ~NE, and the other to ~NE–SW cleavage dipping

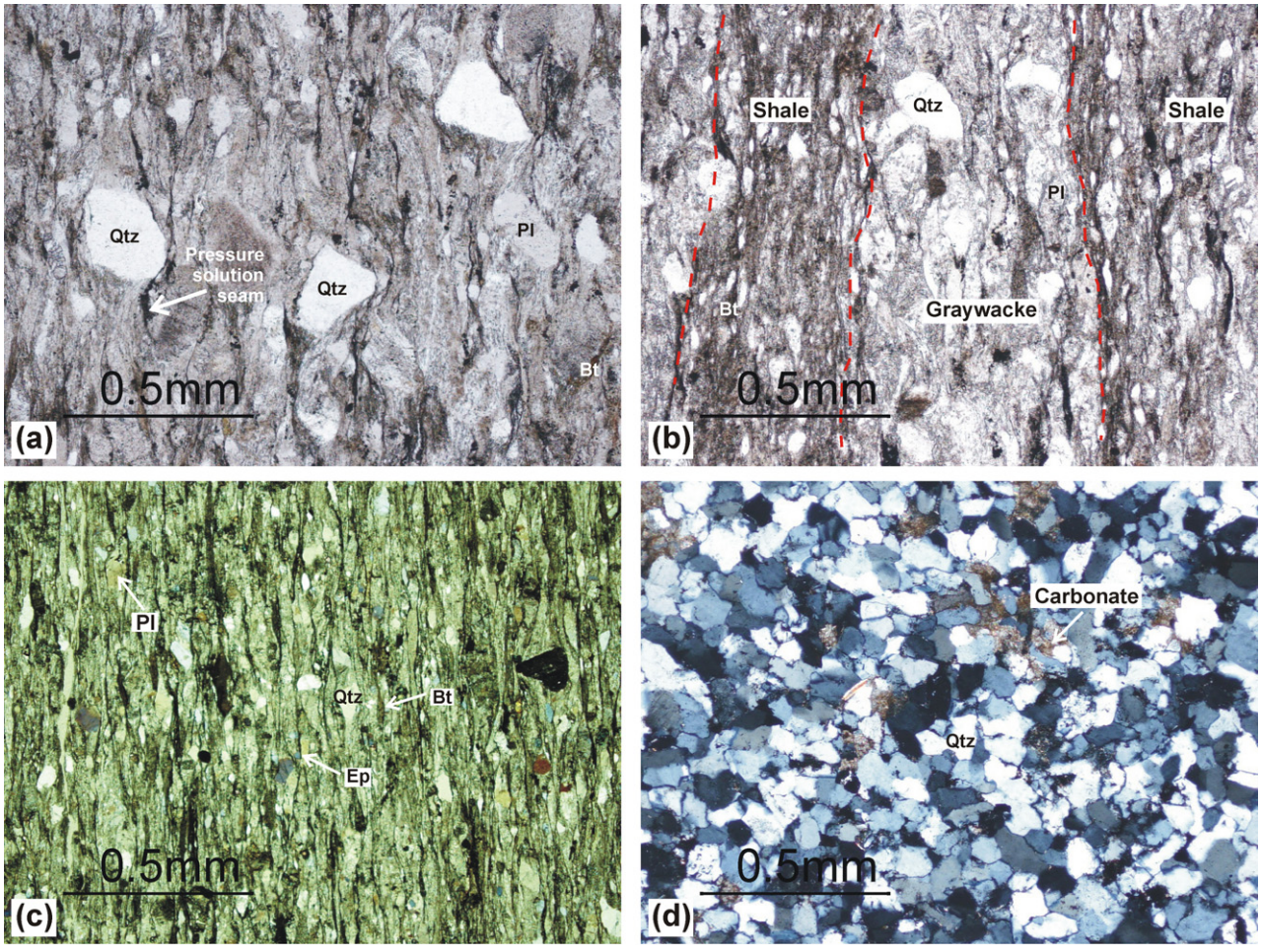

Fig. 11. Microphotographs showing contrasting microstructures and mineral assemblages in (a) Neoproterozoic graywackes in Domain 1, (b) finely laminated graywackes in Domain 2, (c) metagraywackes in Domain 3, and (d) Ordovician quartzite. Mineral symbols and abbreviations after by Kretz (1983), see Fig. 3 for sample locations.

steeply ~SE (Figs. 9 and 10f). Magnetic lineations are subhorizontal but their trends scatter widely (Figs. 9 and 10c).

In summary, the following general trends are revealed by the magnetic fabric survey in the Barrandian Neoproterozoic: (1) The degree of anisotropy (P) varies noticeably from 1.04 (almost isotropic samples) up to 1.31 (Fig. 8b). (2) The shape of the AMS ellipsoid changes significantly from the ~NW to the ~SE, with values of T in both map view (Fig. 9) or AMS plot (Fig. 8b), clearly increasing from Domain 1 to Domain 3, i.e., from prolate through neutral to weakly oblate to significantly oblate AMS ellipsoids. (3) The orientation of the magnetic fabric corresponds well to mesoscopic structures with magnetic foliations having nearly the same orientations as bedding or cleavage and magnetic lineations having similar orientations as lineations measured in outcrop.

6. Microstructures

Microstructures within the Neoproterozoic and Lower Paleozoic rocks were examined at 17 stations along two ~NW–SE transects in order to characterize mineral assemblages, deformation mechanisms, and cleavage development across the three structural domains. Below we describe four representative samples that are typical of each domain and which document a striking microstructural gradient from NW to SE.

6.1. Sample JH7—graywacke from Domain 1

The graywacke is composed chiefly of quartz, plagioclase, K-feldspar, sericite, and partly chloritized clastic biotite (Fig. 11a). The fine-grained quartz and sericite matrix encloses irregularly shaped, subangular detrital porphyroclasts (up to 0.2 mm in size) of feldspar, quartz, and acid volcanic rocks. Quartz is recrystallized in pressure shadows of the porphyroclasts to form grains with significantly reduced grain-size (down to 25 μm). The cleavage is rough and developed as short, discontinuous cleavage domains defined by seams of extremely fine-grained dark material enveloping the large detrital grains (spaced disjunctive cleavage of Powell, 1979; Passchier and Trouw, 2005).

6.2. Sample JH41—graywacke from Domain 2

The main minerals in the sample are quartz, plagioclase, sericite, K-feldspar, and calcite (Fig. 11b). The rock exhibits a weak lamination: laminae composed of large irregular clasts (up to 0.2 mm in size) set in a coarse-grained graywacke matrix alternate with fine-grained silty laminae enclosing significantly smaller detrital grains. The graywacke material is mingled with broken-off shale fragments (presumably micro-scale slump structures; Cháb and Pelc, 1968). Cleavage is largely localized in finer-grained laminae, forming anastomosing but continuous cleavage domains (Fig. 11b).

6.3. Sample JH139—metagraywacke from Domain 3

The metagraywacke is composed of quartz, plagioclase (mostly albite), biotite, muscovite, chlorite, epidote and actinolite, with titanite and microcline as accessory minerals (Fig. 11c). Acicular actinolite has grown at the expense of detrital hornblende in the pressure shadows of quartz and feldspar porphyroclasts. Such a mineral assemblage indicates lower greenschist facies conditions with stable chlorite, albite, epidote, and actinolite. The metagreywacke also contains flattened clasts of black shale, siltstone, and devitrified volcanic glass. No sedimentary textures are preserved. Instead, the rock has been penetratively deformed by closely spaced smooth to anastomosing (around larger subangular grains) cleavage domains defined by ultra-fine-grained dark seams wrapping around larger grains (Fig. 11c). The cleavage is enhanced by the alignment of biotite grains and flattened siltstone clasts in the microlithons.

In the Neoproterozoic rocks, the deformational microstructures are characterized by increasing volume and smoothness of cleavage domains from the NW to the SE. In addition, the degree of regional metamorphism increases to the SE as documented by syntectonic growth of chlorite and epidote in Domains 2 and 3.

6.4. Sample JH28—undeformed Ordovician quartzite

The rock is well-sorted, composed predominantly of quartz with almost no matrix preserved. Calcite and tourmaline occur as accessory minerals (Fig. 11d). The quartz grains, approximately 0.1 mm in size, have irregular boundaries and show only weak undulatory extinction (Fig. 11d). In contrast to the Neoproterozoic rocks, the quartzite is virtually undeformed with no micro-scale evidence for recrystallization or cleavage.

7. Discussion

7.1. Criteria used to separate Cadomian from Variscan deformation

The following criteria firmly establish the Cadomian age of deformation structures (described above) in the Neoproterozoic basement along the northwestern margin of the Barrandian area. (1) An angular unconformity exists between the steep pervasive cleavage in the Neoproterozoic slates developed under prehnite–pumpellyite to lower greenschist facies conditions (Cháb and Bernardová, 1974; Cháb et al., 1995; this study) and the only gently to moderately tilted and internally unstrained Middle Cambrian and Ordovician strata (Fig. 7a). (2) The ?Cambro–Ordovician felsic dikes cut across the cleavage with knife-sharp discordant contacts and also enclose wall-rock xenoliths with cleavage (Fig. 7b). (3) The angular unconformity between the cleavage in the Neoproterozoic rocks and bedding in the Lower Paleozoic rocks is expressed both at map-scale (Fig. 5) and in the mean directions calculated from the structural data. In Domain 3, the cleavage is folded about an 038°-trending axis that makes an angle of 29° to the mean strike of the overlying Lower Paleozoic strata (067°). (4) The 40° angular divergence exists between the mean Lower Paleozoic fold axis and conjugate kink bands superposed on the flat-lying cleavage (Fig. 7d and e; mean strike of kink axial planes is 027°). (5) The Middle Cambrian and Lower Ordovician strata and Cambro–Ordovician extrusive rocks of the Křivoklát–Rokycany volcanic complex (KRVC in Fig. 5), which overlap the structural domains (Domains 1–3), constrain the age of early movements along the boundary faults and domain juxtaposition to the pre-Middle Cambrian. In general, however, the ~NE–SW faults in the Cadomian basement (presumably including the Domains 1–3 boundaries) may have been later reactivated during Early Paleozoic basin formation and subsequent Variscan structural inversion (Chlupáč et al., 1998).

In contrast to the above, Variscan deformation recorded in the adjacent Lower Paleozoic rocks is non-penetrative and characterized by a simple fold style. Variscan folding resulted only in moderate tilting of the bedding in the Lower Ordovician siliciclastic rocks to the SE about a 067°-trending axis (Fig. 5), and in the reorientation (steepening) of the Cadomian cleavage and kink-bands superposed onto the cleavage in the adjacent Neoproterozoic basement (Fig. 5).

7.2. Tectonic model for the Teplá–Barrandian Neoproterozoic accretionary wedge

As summarized in Table 1, the three structural domains defined in this paper differ significantly in lithology, style and intensity

Table 1
Characteristics of structural domains (Domains 1–3) and overlying Lower Paleozoic rocks along the northwestern margin of the Barrandian area. Lithostratigraphy after [a]Mašek (2000), [b]Holubec (1995), [c]Röhlich (1965), [d]Cháb and Pelc (1968).

Domain	Lithology	Stratigraphy	Structures					Mineral assemblage
			Bedding	Cleavage	Magnetic foliation	Magnetic lineation	AMS ellipsoid	
1	Flysch-like alternating graywackes and shales	Blovice Fm.[a]	(1) ~ENE–WSW	Spaced disjunctive, bedding-parallel	Moderate to steep dip to the ~N–NW	Shallow plunge to the ~W–WSW	Prolate	Weak burial metamorphism Qtz, Plg, Kfs, Ser
		Rakovník G.[b] Kralovice–Rakovník belt[c] Flysch facies[d]	(2) ~NE–SW					
2	Graywackes and slates, olistoliths, slump structures, basalt bodies	Blovice Fm.[a]	Variable, ~E–W dominant	Anastomosing, continuous	Moderate dip to the ~NE	Three distinct orientations, dominant lineation plunges shallowly to the ~NNW	Neutral to weakly oblate	Prehnite–pumpellyite to lower greenschist facies
		Zvíkovec G.[b]		~ENE–WSW to ~ESE–WNW				Qtz, Plg, Kfs, Ser, Chl, Ep
		Radnice–Kralupy belt[c] Volcanogenic facies[d]		(2) ~ENE–WSW to ~ESE–WNW				
3	Slates, graywackes, chert lenses	Blovice Fm.[a]	No bedding preserved due to pervasive deformation	Smooth, poles create a girdle around axis 38°/17°, cleavage steepens near the contact with Lower Paleozoic	Gentle dip to the ~NE	Subhorizontal with variable trend, dominant ~SSE	Oblate	Prehnite–pumpellyite to lower greenschist facies
		Úslava G.[b]						Qtz, Plg, Kfs, Ser, Chl, Ep, Mu, Amp
		Zbiroh–Šárka belt[c] Monotonous facies[d]						
Barrandian Lower Paleozoic	Shales, siltstones, sandstones, basalts, andesites	Lower Ordovician	Homogeneously oriented, mean strike 66°, dip to the ~SSE	No cleavage or bedding-parallel cleavage in shale interbeds	No data	No data	No data	Clastic grains, no metamorphic minerals

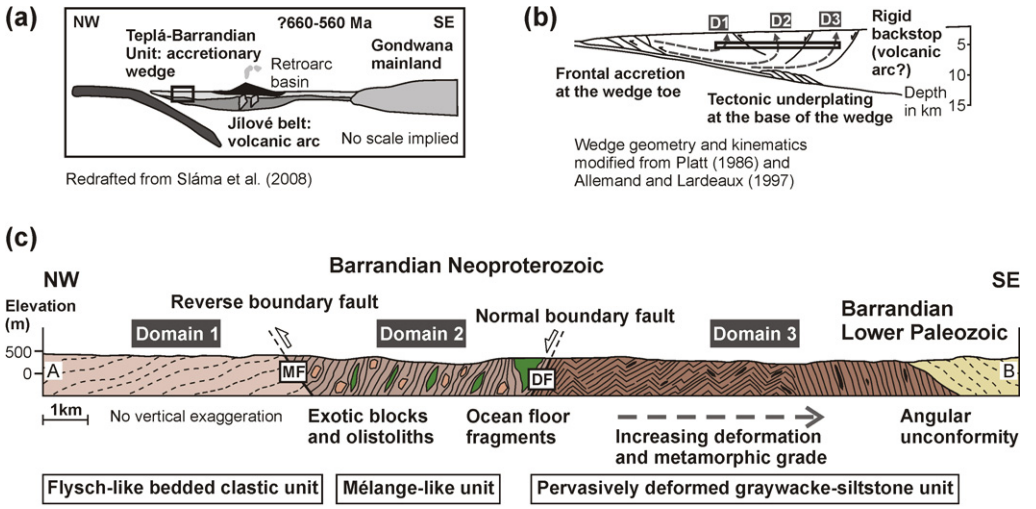

Fig. 12. Tentative tectonic model for the NW flank of the Teplá–Barrandian unit as a Cadomian accretionary wedge between a subduction zone to the NW and a volcanic arc to the SE (present-day coordinates). (a) Interpretation of an overall geotectonic setting of the Teplá–Barrandian unit during Cadomian orogeny after Sláma et al. (2008). Bold rectangle indicates presumed position of the study area. (b) Simplified Platt (1986) kinematic model for an accretionary wedge showing inferred position and differential burial–exhumation trajectories (dashed gray lines) of the three structural domains (D1–D3) described in this paper. Bold rectangle represents interpreted position of cross-section in (c). (c) Simplified interpretive cross-section along line A–B (location shown in Fig. 3). The three structural domains are interpreted to represent contrasting units juxtaposed within the accretionary wedge along localized boundary faults. The total amount of displacement and exact timing of movements along the boundary faults are unknown. DF: Družec fault, MF: Městečko fault.

of deformation, and degree of Cadomian regional metamorphism. The amount of finite shortening, as revealed by cleavage intensity and progressive flattening of the AMS ellipsoid, and temperature conditions of deformation generally increase to the SE from prehnite–pumpellyite up to lower greenschist facies conditions ($T \sim 250$–$350\,^{\circ}$C; Cháb and Bernardová, 1974; Suchý et al., 2007). Based on these data and the newly defined lithotectonic zonation we propose the following kinematic model for the TBU accretionary wedge during the Cadomian orogeny (Fig. 12). We adopt the paleo-subduction zone polarity and timing of deformation events proposed by Dörr et al. (2002) and Sláma et al. (2008), which are consistent with our structural data (Fig. 12a).

The northwesterly Domain 1 is both the most outboard (trenchward) unit. It has never been significantly buried within the wedge (Fig. 12b) and experienced only weak deformation and folding. Both the tilt of the bedding to the ~NW and the bedding-parallel low-temperature cleavage formed by pressure solution in slate interbeds are the result of flexural-slip folding. The cleavage is associated with an ~E–W magnetic lineation and prolate shapes of the AMS ellipsoid (Figs. 8b and 9). In terms of orientation, the magnetic lineation corresponds to the mesoscopic lineation and both are interpreted to represent the bedding-oblique flexural-slip direction. Compared to the slate interbeds, the internal strain recorded by the graywackes during flexural-slip folding was weak since the degree of anisotropy P is generally low.

In contrast to Domain 1, the central mélange-like Domain 2 is characterized by heterogenous intense deformation and predominantly ~E–W relic bedding and cleavage associated with neutral shapes of the AMS ellipsoids (Figs. 8b and 9). Mesoscopic lineation is almost absent, suggesting a flattening strain associated with the cleavage development. The magnetic lineation is interpreted to represent the intersection of mesoscopic cleavage and bedding and presumably corresponds to the common axis of phyllosilicate grains in various stages of reorientation. This interpretation is consistent with the lack of mesoscopic stretching lineation and absence of evidence for flexural slip. Thus, the AMS lineations cannot represent a mineral (stretching) lineation (e.g., Parés and van der Pluijm, 2002). Magnetic foliations correspond to the cleavage, both recording heterogenous deformation during dominantly ~N–S shortening. Syntectonic growth of chlorite along cleavage planes suggests increased regional metamorphism (prehnite–pumpellyite to lower greenschist facies conditions) relative to Domain 1 (Fig. 12b).

Hence, we envision the evolution of central Domain 2 as involving: (1) graywacke-argillite mélange formation by the mingling of broken-off sedimentary rocks and pieces of ocean floor, (2) burial to depths corresponding to prehnite–pumpellyite to lower greenschist facies conditions, and (3) later heterogenous ductile deformation with dominant ~N–S shortening. The mélange formation and heterogeneous deformation may have taken place in the subduction channel (e.g., Cloos, 1982; Cowan, 1985; Cloos and Shreve, 1988a,b), however, the weak ~N–S shortening is also recorded in graywackes of Domain 1 at higher structural levels. Subsequently, Domain 2 was exhumed and thrust over Domain 1 as a rigid block along a highly localized ~NE–SW-trending fault (Figs. 7f and 12b and c).

The most inboard (arcward) but lithologically monotonous Domain 3 was also buried to depths corresponding to the lower greenschist facies conditions (indicated by the syntectonic growth of epidote, actinolite and albite; Fig. 11c) where it was pervasively overprinted by flattening strain as evidenced by an intensely developed, ~SE-dipping cleavage and oblate AMS ellipsoids (Figs. 8b and 9). Continued shortening produced contractional kink-bands and chevron folds (Fig. 7c and d) superimposed on the greenschist-facies cleavage. Exhumation of Domain 3 was accommodated by a major ~NE–SW normal fault (Figs. 7g and 12b and c).

Taken together, we interpret this structural history to record discrete deformational events and differential exhumation of the three structural domains from various depths within the accretionary wedge during active subduction in a manner analogous to that theoretically elaborated by Platt (1986). The NW-directed thrusting of Domain 2 over Domain 1 is thought to have been caused by accretion at the wedge front, whereas the SE-dipping cleavage and exhumation of Domain 3 is interpreted to record inclined pervasive shortening during tectonic underplating and subsequent horizontal extension of the rear of the wedge (Fig. 12b; e.g., Platt, 1986; Cloos and Shreve, 1988a,b; Allemand and Lardeaux, 1997). It is important to note, however, that the exact timing of these processes is unknown and that the structural history of the wedge was likely much more complex (e.g., Braid et al., in press).

Combining our structural data with recent high-precision geochronology (Sláma et al., 2008), we suggest that the overall convergent setting and intraoceanic subduction-driven processes lasted from ?660–560 Ma as recorded in the Kralupy–Zbraslav Group, although the main phase of shortening was coeval with syntectonic flysch sedimentation at ~560–530 Ma (Sláma et al., 2008). In the overlying flysch succession of the Štěchovice Group (Fig. 2), clastic material was derived from both the arc and the nearby continental crust (Sláma et al., 2008), suggesting telescoping of the accretionary wedge–arc system between an arriving aseismic ridge or oceanic plateau to the N or NW and a rigid backstop to the SE (?continental basement; Figs. 1d and 12a). The syntectonic flysch sedimentation continued until ~530 Ma in a southeasterly short-lived retroarc basin (Sláma et al., 2008). The deformation and sedimentation thus progressively migrated in the wedge/arc system from the NW to the SE, i.e., towards the presumed continent (Gondwana mainland in Fig. 12a). Boninite dikes cutting across the graywackes contain ~540 Ma zircons and are overlain by Middle Cambrian strata, suggesting that the mid-ocean ridge entered the trench and caused anomalous thermal conditions in the overriding lithospheric mantle.

A more precise paleogeographic reconstruction of the original subduction zone geometry, accretionary wedge width, and extent of the volcanic arc is, unfortunately, hindered by extensive Variscan (Late Devonian to Early Carboniferous) reworking of the TBU margins and possible rotations of the entire TBU block (e.g., Edel et al., 2003).

7.3. Comparison of the Teplá–Barrandian unit with related Cadomian terranes

Since the TBU is a component of the Cadomian–Avalonian belt with affinities to the Armorican Terrane Assemblage (e.g., Tait et al., 1997; Franke and Zelazniewicz, 2002; Drost et al., 2004, 2007; Kalvoda et al., 2008; Sláma et al., 2008), we briefly compare its tectonic evolution to that of the two geologically most closely related terranes (the adjacent Saxothuringia and the Armorica s.s.; Fig. 1a), emphasizing the main differences in order to highlight the uniqueness of some aspects of the TBU.

The Neoproterozoic basement of the Saxothuringian unit (exposed in the Lausitz block and North Saxon Anticline) comprises three lithotectonic units interpreted as a backarc basin, a retroarc basin with a related remnant basin, and a shelf-basin with passive-margin deposits (e.g., Linnemann and Romer, 2002; Buschmann et al., 2006; Linnemann et al., 2007, 2008a,b,c). Accretionary wedge sediments and a related magmatic arc have not been preserved, but the existence of an arc is reflected in the composition of the backarc basin sediments. A recent tectonic model proposed by Linnemann et al. (2007) for the Saxothuringian unit assumes the co-existence of a magmatic arc, backarc basin, and a passive margin during subduction at ~570 Ma, followed by a collision of the arc with the continent, and subsequent closure of backarc basin to form a fold-and-thrust belt with related retroarc basin at ~543 Ma (see Figs. 13 and 14 in Linnemann et al., 2007). The final stages of the Cadomian orogeny were accompanied by intrusions of granitoid plutons into the sedimentary successions at ~570–560 Ma and ~540–530 Ma.

The North Armorican Massif (Armorica s.s.), a classic area where the Cadomian orogeny was first defined (Bertrand, 1921), is an assemblage of four terranes separated by steep ductile shear zones and brittle faults (e.g., Strachan et al., 1989; D'Lemos et al., 1990; Treloar and Strachan, 1990; Brown, 1995; Miller et al., 1999; Ballévre et al., 2001; Chantraine et al., 2001; Samson et al., 2005; Linnemann et al., 2008b). The most outboard (northwestern) part of the Massif is made up of ~2 Ga Icartian basement, interpreted as a detached fragment of the West African Craton, and a volcanic arc built on this basement (Samson et al., 2005; Linnemann et al., 2008b). The accretionary wedge is not exposed, but is assumed to lie offshore further to the N. To the S, sediments of an intra-arc basin and magmatic rocks that lack an ancient basement are present (Linnemann et al., 2008b). The two southernmost terranes represent a backarc basin with LP–HT metamorphic rocks and numerous granitoid plutons, and are separated from the Central Armorican Massif by the Variscan North Armorican Shear Zone. A tectonic model proposed for these terranes invokes oblique subduction of an aseismic ridge or island arc at ~610 Ma beneath an active continental margin, leading to segmentation of the margin, sinistral transpression, and intracrustal melting producing migmatites and granitoids in the backarc region (Brown, 1995).

Comparison of the TBU with these two regions shows that subduction, arc magmatism, and regional deformation broadly overlapped in time along the Cadomian active margin. But there are several striking differences: (1) Pre-Cadomian continental basement is not exposed in the TBU, contrary to the ~2 Ga Icartian gneisses of the Armorican Massif. Instead, seismic anisotropy data indicate the TBU to be underlain by attenuated mantle lithosphere with its own mantle fabric distinct from that of adjacent units (Babuška et al., in press). In addition, seismic profiles show significant subhorizontal to SSE-dipping reflections in the TBU at depth, a seismic pattern similar to subduction–accretion complexes in modern arcs (Tomek et al., 1997). The geophysical data are thus consistent with the presumed accretionary wedge model for the TBU during the Cadomian orogeny. (2) Unlike the Armorican Massif, backarc volcanic complexes, LP–HT metamorphic core complexes, and extensive granitoid magmatism have not been found in association with the Cadomian evolution of the TBU. This would suggest a rather limited amount of backarc extension, perhaps due to flat-slab subduction. (3) In both the North Armorican Massif and Saxothuringia, oblique Cadomian subduction of oceanic lithosphere is assumed, producing large-scale strike-slip shear zones separating individual lithotectonic units. In contrast, no evidence has been found in the TBU for significant Cadomian strike-slip movements, suggesting frontal subduction with the trenchward margin of the TBU oriented at a high angle to the subduction vector in this part of the Cadomian belt.

8. Conclusions

(1) Three contrasting lithotectonic units (Domains 1–3) occur in the central part of the TBU that differ in lithology (flysch-like, graywacke–argillite mélange with pieces of ocean floor, and monotonous siliciclastic), style and intensity of deformation, magnetic fabric, and in the degree of regional metamorphism. The amount of finite shortening and the temperature conditions of deformation generally increase from the NW to the SE across these units, i.e., from the unmetamorphosed Domain 1 to the lower greenschist facies Domain 3.

(2) The boundaries between the adjacent domains are major antithetic brittle faults: the Domain 1/2 boundary is a thrust fault associated with top-to-the-NW movement (Domain 2 over Domain 1), whereas the Domain 2/3 boundary is a normal fault (Domain 2 down, Domain 3 up). The domains are overstepped by the Middle Cambrian and Lower Ordovician successions and Cambro–Ordovician volcanic rocks, constraining the age for domain juxtaposition and early movements along the boundary faults to the pre-Middle Cambrian (Late Cadomian).

(3) We interpret Domains 1–3 as allochtonous tectonic slices of an accretionary wedge at the northern active margin of Gondwana during the Late Neoproterozoic Cadomian orogeny (~660–540 Ma) that were differentially exhumed from various depths within the wedge during subduction. The NW-directed thrusting of Domain 2 over the most outboard Domain 1 may

have been caused by accretion at the wedge front, whereas the exhumation of the arcward Domain 3 may record shortening during underplating and subsequent extension at the rear of the wedge. This model may also explain the uplift and erosion of older sedimentary rocks of the Kralupy–Zbraslav Group and volcanic arc rocks of the Jílové Belt, and the shift of sedimentation to the SE, where a small retroarc basin formed during the terminal Neoproterozoic/Early Cambrian. The intrusion of boninite dikes bracketed between ~540 and 520 Ma may reflect the ridge–trench collision and the transition from destructive to transform margin during Early/Middle Cambrian. Such a kinematic scenario would suggest that the Cadomian wedges developed in a manner identical to Phanerozoic and modern accretionary margins.

(4) Compared to related Armorican-type terranes, the TBU lacks exposed continental basement, evidence for strike-slip shearing, extensive backarc plutonism and LP–HT metamorphism and anatexis, which could be interpreted as a result of frontal flat-slab Cadomian subduction.

(5) Finally, our study emphasizes that the TBU may represent the best preserved fragment of an accretionary wedge in the entire Avalonian–Cadomian belt and may therefore provide unique insight into the style, kinematics, and timing of accretionary processes along the Avalonian–Cadomian belt. Further research should focus on the larger-scale kinematic pattern linked to a petrologic study of regional metamorphism to better understand the details of the P–T evolution of different segments of the wedge, and on precise geochronology of the volcanic rocks in Domains 1–3 to reconstruct their stratigraphic relations as a time constraint for tectonic models.

Acknowledgements

We gratefully acknowledge the very constructive and thorough reviews by R. Damian Nance and Ulf Linnemann; their comments and suggestions helped improve the original manuscript significantly. We also thank Oldřich Fatka for discussions and František Hrouda for assistance in measuring AMS at AGICO Inc., Brno, Czech Republic. This study is a part of Ph.D. research of Jaroslava Hajná, supported by Grant No. 134908 from the Grant Agency of Charles University in Prague (GAUK) to J. Hajná, and by the Ministry of Education, Youth and Sports of the Czech Republic Research Plan No. MSM0021620855. Part of the research was carried out under the framework of the Academic Research Plan AV0Z30130516 of Institute of Geology, Academy of Sciences of the Czech Republic, v.v.i.

Appendix A. Supplementary data

Supplementary data associated with this article can be found, in the online version, at doi:10.1016/j.precamres.2009.10.009.

References

Allemand, P., Lardeaux, J.M., 1997. Strain partitioning and metamorphism in a deformable orogenic wedge: application to the Alpine belt. Tectonophysics 280, 157–169.

Babuška, V., Fiala, J., Plomerová, J., in press. Bottom to top lithosphere structure and evolution of western Eger Rift (Central Europe). Int. J. Earth Sci., doi:10.1007/s00531-009r-r0434-4.

Ballévre, M., Le Goff, E., Hébert, R., 2001. The tectonothermal evolution of the Cadomian belt of northern Brittany, France: a Neoproterozoic volcanic arc. Tectonophysics 331, 19–43.

Bertrand, L., 1921. Les anciennes mers de la France et leurs depots. Flammarion, Paris, 190 pp.

Braid, J.A., Murphy, B.J., Quesada, C., in press. Structural analysis of an accretionary prism in a continental collisional setting, the Late Paleozoic Pulo do Lobo Zone, Southern Iberia. Gondwana Res., doi:10.1016/j.gr.2009.09.003.

Brown, M., 1995. The late-Precambrian geodynamic evolution of the Armorican segment of the Cadomian belt (France): distortion of an active continental margin during south-west directed convergence and subduction of a bathymetric high. Géol. France 3, 3–22.

Buschmann, B., Elicki, O., Jonas, P., 2006. The Cadomian unconformity in the Saxo–Thuringian Zone, Germany: palaeogeographic affinities of Ediacaran (terminal Neoproterozoic) and Cambrian strata. Precambrian Res. 147, 387–403.

Cháb, J., 1993. General problems of the TB (Teplá–Barrandian) Precambrian, Bohemian Massif, the Czech Republic. Bull. Geosci. 68, 1–6.

Cháb, J., Bernardová, E., 1974. Prehnite and pumpellyite in the Upper Proteroyoic basalts of the north-western part of the Barrandian region (Czechoslovakia). Krystalinikum 10, 53–66.

Cháb, J., Pelc, Z., 1968. Lithology of Upper Proterozoic in the NW limb of the Barrandian area. Krystalinikum 6, 141–167.

Cháb, J., Suchý, V., Vejnar, Z., 1995. Metamorphic evolution (the Teplá–Barrandian Zone). In: Dallmeyer, R.D., Franke, W., Weber, K. (Eds.), Pre-Permian Geology of Central and Eastern Europe. Springer-Verlag, Berlin/Heidelberg/New York, pp. 392–397.

Chadima, M., Pruner, P., Šlechta, S., Grygar, T., Hirt, A.M., 2006. Magnetic fabric variations in Mesozoic black shales, Northern Siberia, Russia: possible paleomagnetic implications. Tectonophysics 418, 145–162.

Chaloupský, J., Chlupáč, I., Mašek, J., Waldhausrová, J., Cháb, J., 1995. Stratigraphy of the Teplá–Barrandian zone (Bohemicum). In: Dallmeyer, R.D., Franke, W., Weber, K. (Eds.), Pre-Permian Geology of Central and Eastern Europe. Springer, Berlin/Heidelberg/New York, pp. 379–391.

Chantraine, J., Egal, E., Thieblemont, D., Le Goff, E., Guerrot, C., Ballévre, M., Guennoc, P., 2001. The Cadomian active margin (North Armorican Massif, France): a segment of the North Atlantic Panafrican belt. Tectonophysics 331, 1–18.

Chlupáč, I., Havlíček, V., Kříž, J., Kukal, Z., Štorch, P., 1998. Palaeozoic of the Barrandian (Cambrian–Devonian). Czech Geological Survey, Prague, 183 pp.

Cloos, M., 1982. Flow melanges: numerical modeling and geologic constraints on their origin in the Franciscan subduction complex. Geol. Soc. Am. Bull. 93, 330–345.

Cloos, M., Shreve, R.L., 1988a. Subduction-channel model of prism accretion, melange formation, sediment subduction, and subduction erosion at convergent plate pargins: 1. Background and description. PAGEOPH 128, 455–500.

Cloos, M., Shreve, R.L., 1988b. Subduction-channel model of prism accretion, melange formation, sediment subduction, and subduction erosion at convergent plate margins: 2. Implications and discussion. PAGEOPH 128, 501–545.

Cocks, L.R.M., Torsvik, T.H., 2002. Earth geography from 500 to 400 million years ago. A faunal and palaeomagnetic review. J. Geol. Soc. London 159, 631–644.

Cowan, D.S., 1974. Deformation and metamorphism of the Franciscan subduction zone complex northwest of Pacheco Pass, California. Geol. Soc. Am. Bull. 85, 1623–1634.

Cowan, D.S., 1985. Structural styles in Mesozoic and Cenozoic melanges in the Western Cordillera of North America. Geol. Soc. Am. Bull. 96, 451–462.

Dallmeyer, R.D., Urban, M., 1998. Variscan vs Cadomian tectonothermal activity in northwestern sectors of the Teplá–Barrandian zone, Czech Republic: constraints from $^{40}Ar/^{39}Ar$ ages. Geol. Rundsch. 87, 94–106.

D'Lemos, R.S., Strachan, R.A., Topley, C.G., 1990. The Cadomian Orogeny in the North Armorican Massif: a brief review. In: D'Lemos, R.S., Strachan, R.A., Topley, C.G. (Eds.), The Cadomian Orogeny, vol. 51. Geol. Soc. London Spec. Publ., pp. 3–12.

Dörr, W., Zulauf, G., in press. Elevator tectonics and orogenic collapse of a Tibetan-style plateau in the European Variscides: the role of the Bohemian shear zone. Int. J. Earth Sci., doi:10.1007/s00531-008-0389-x.

Dörr, W., Fiala, J., Vejnar, Z., Zulauf, G., 1998. U–Pb zircon ages and structural development of metagranitoids of the Teplá crystalline complex—evidence for pervasive Cambrian plutonism within the Bohemian Massif (Czech Republic). Geol. Rundsch. 87, 135–149.

Dörr, W., Zulauf, G., Fiala, J., Franke, W., Vejnar, Z., 2002. Neoproterozoic to Early Cambrian history of an active plate margin in the Teplá–Barrandian unit—a correlation of U–Pb isotopic-dilution-TIMS ages (Bohemia, Czech Republic). Tectonophysics 352, 65–85.

Dostal, J., Patočka, F., Pin, C., 2001. Middle/Late Cambrian intracontinental rifting in the central West Sudetes, NE Bohemian Massif (Czech Republic): geochemistry and petrogenesis of the bimodal metavolcanic rocks. Geol. J. 36, 1–17.

Drost, K., Linnemann, U., McNaughton, N., Fatka, O., Kraft, P., Gehmlich, M., Tonk, Ch., Marek, J., 2004. New data on the Neoproterozoic–Cambrian geotectonic setting of the Teplá–Barrandian volcano-sedimentary successions: geochemistry, U–Pb zircon ages, and provenance (Bohemian Massif, Czech Republic). Int. J. Earth Sci. 93, 742–757.

Drost, K., Romer, R.L., Linnemann, U., Fatka, O., Kraft, P., Marek, J., 2007. Nd–Sr–Pb isotopic signatures of Neoproterozoic—early Paleozoic siliciclastic rocks in response to changing geotectonic regimes: a case study from the Barrandian area (Bohemian Massif, Czech Republic). In: Linnemann, U., Nance, D., Kraft, P., Zulauf, G. (Eds.), The Evolution of the Rheic Ocean: From Avalonian–Cadomian Active Margin to Alleghenian–Variscan Collision. Geol. Soc. Am. Spec. Paper 423, pp. 191–208.

Dubanský, A., 1984. Determination of the radiogenic age by the K–Ar method (geochronological data from the Bohemian Massif in the ČSR region). Sbor. Věd. prací Vys. šk. báňské 30, 137–170 (in Czech).

Edel, J.B., Schulmann, K., Holub, F.V., 2003. Anticlockwise and clockwise rotations of the Eastern Variscides accommodated by lithospheric wrenching: palaeomagnetic and structural evidence. J. Geol. Soc. London 160, 209–218.

Fatka, O., Gabriel, Z., 1991. Microbiota from siliceous stromatolitic rocks of the Barrandian Proterozoic (Bohemian Massif). J. Min. Geol. 36, 143–148.

Fiala, F., 1977. The Upper Proterozoic volcanism of the Barrandian area and the problem of spilites. J. Geol. Sci., Geol. 30, 2–247.
Franke, W., Zelazniewicz, A., 2002. Structure and evolution of the Bohemian arc. In: Winchester, J.A., Pharaoh, T.C., Verniers, J. (Eds.), Palaeozoic amalgamation of Central Europe, vol. 201. Geol. Soc. London Spec. Publ., pp. 279–293.
Geyer, G., Elicki, O., Fatka, O., Zylinska, A., 2008. Cambrian. In: McCann, T. (Ed.), The Geology of Central Europe, vol. 1: Precambrian and Palaeozoic. Geological Society, London, pp. 155–202.
Holubec, J., 1995. Structure (the Teplá–Barrandian Zone). In: Dallmeyer, R.D., Franke, W., Weber, K. (Eds.), Pre-Permian Geology of Central and Eastern Europe. Springer-Verlag, Berlin/Heidelberg/New York, pp. 392–397.
Hrouda, F., 1982. Magnetic anisotropy of rocks and its application in geology and geophysics. Geophys. Surv. 5, 37–82.
Hsü, K.J., 1968. Principles of mélanges and their bearing on the Franciscan-Knoxville paradox. Geol. Soc. Am. Bull. 79, 1063–1074.
Jakeš, P., Zoubek, J., Zoubková, J., Franke, W., 1979. Graywackes and metagraywackes of the Teplá–Barrandian proterozoic area. J. Geol. Sci., Geol. 33, 83–122.
Jelínek, V., 1981. Characterization of magnetic fabric of rocks. Tectonophysics 79, 563–567.
Kachlík, V., Patočka, F., 1998. Cambrian/Ordovician intracontinental rifting and Devonian closure of the rifting generated basins in the Bohemian Massif realms. Acta Univ. Carol., Geol. 42, 433–441.
Kalvoda, J., Bábek, O., Fatka, O., Leichmann, J., Melichar, R., Nehyba, S., Špaček, P., 2008. Brunovistulian terrane (Bohemian Massif, Central Europe) from late Proterozoic to late Paleozoic: a review. Int. J. Earth Sci. 97, 497–518.
Kettner, R., 1923. Cambrian of the Skreje–Tejřovice area. Sbor. Stát. geol. Úst. Čs. Republ. 3, 5–63 (in Czech).
Kettner, R., Slavík, F., 1929. New section through Algonkian and Cambrian near Tejřovice. Rozpravy II. třídy České akademie věd 38, 1–30 (in Czech).
Košler, J., Bowes, D.R., Farrow, C.M., Hopgood, A.M., Rieder, M., Rogers, G., 1997. Constraints on the timing of events in the multi-episodic of the Teplá–Barrandian complex, western Bohemia, from integration of deformational sequence and Rb–Sr isotopic data. N. Jb. Miner., Mh. 5, 203–220.
Kretz, R., 1983. Symbols for rock forming minerals. Am. Miner. 68, 277–279.
Kříbek, B., Pouba, Z., Skoček, V., Waldhausrová, J., 2000. Neoproterozoic of the Teplá–Barrandian Unit as a part of the Cadomian orogenic belt: a review and correlation aspects. Bull. Czech Geol. Surv. 75, 175–196.
Krs, M., Krsová, M., Pruner, P., Chvojka, R., Havlíček, V., 1987. Palaeomagnetism, palaeogeography and the multicomponent analysis of middle and upper Cambrian rocks of the Barrandian in the Bohemian Massif. Tectonophysics 139, 1–20.
Krs, M., Pruner, P., Man, O., 2001. Tectonic and paleogeographic interpretation of the paleomagnetism of Variscan and pre-Variscan formations of the Bohemian Massif, with special reference to the Barrandian terrane. Tectonophysics 332, 93–114.
Lang, M., 2000. Composition of Proterozoic greywackes in the Barrandian. Bull. Czech Geol. Surv. 75, 205–216.
Linnemann, U., Romer, R.L., 2002. The Cadomian orogeny in Saxo-Thuringia, Germany: geochemical and Nd–Sr–Pb isotopic characterization of marginal basins with constraints to geotectonic setting and provenance. Tectonophysics 352, 33–64.
Linnemann, U., McNaughton, N.J., Romer, R.L., Gehmlich, M., Drost, K., Tonk, C., 2004. West African provenance for Saxo-Thuringia (Bohemian Massif): did Armorica ever leave pre-Pangean Gondwana? U/Pb-SHRIMP zircon evidence and the Nd-isotopic record. Int. J. Earth Sci. 93, 683–705.
Linnemann, U., Gerdes, A., Drost, K., Buschmann, B., 2007. The continuum between Cadomian orogenesis and opening of the Rheic Ocean: constraints from LA-ICP-MS U–Pb zircon dating and analysis of plate-tectonic setting (Saxo-Thuringian zone, northeastern Bohemian Massif, Germany). In: Linnemann, U., Nance, D., Kraft, P., Zulauf, G. (Eds.), The Evolution of the Rheic Ocean: From Avalonian–Cadomian active margin to Alleghenian–Variscan Collision. Geol. Soc. Am. Spec. Paper 423, pp. 61–96.
Linnemann, U., Pereira, F., Jeffries, T.E., Drost, K., Gerdes, A., 2008a. The Cadomian orogeny and the opening of the Rheic Ocean: the diacrony of geotectonic processes constrained by LA-ICP-MS U–Pb zircon dating (Ossa-Morena and Saxo-Thuringian Zones, Iberian and Bohemian Massifs). Tectonophysics 461, 21–43.
Linnemann, U., D'Lemos, R.S., Drost, K., Jeffries, T., Gerdes, A., Romer, R.L., Samson, S.D., Strachan, R.A., 2008b. Cadomian tectonics. In: McCann, T. (Ed.), The Geology of Central Europe, vol. 1: Precambrian and Palaeozoic. Geological Society, London, pp. 103–154.
Linnemann, U., Drost, K., Elicki, O., Gaitzsch, B., Gehmlich, M., Hahn, T., Kroner, U., Romer, R.L., 2008c. Das Saxothuringikum. Museum für Mineralogie und Geologie, Dresden, 163 pp.
Martín-Hernández, F., Hirt, A.M., 2003. The anisotropy of magnetic susceptibility in biotite, muscovite and chlorite single crystals. Tectonophysics 367, 13–28.
Mašek, J., 2000. Stratigraphy of the Proterozoic of the Barrandian area. Bull. Czech Geol. Surv. 75, 197–200.
McCann, T. (Ed.), 2008. The Geology of Central Europe, vol. 1: Precambrian and Palaeozoic. Geological Society, London, 748 pp.
Miller, B.V., Samson, S.D., D'Lemos, R.S., 1999. Time span of plutonism, fabric development, and cooling in a Neoproterozoic magmatic arc segment: U–Pb age constraints from syn-tectonic plutons, Sark, Channel Islands, UK. Tectonophysics 312, 79–95.
Murphy, J.B., Eguiluz, L., Zulauf, G., 2002. Cadomian orogens, peri-Gondwanan correlatives and Laurentia–Baltica connections. Tectonophysics 352, 1–9.
Murphy, J.B., Pisarevsky, S.A., Nance, R.D., Keppie, J.D., 2004. Neoproterozoic–Early Paleozoic evolution of peri-Gondwanan terranes: implications for Laurentia–Gondwana connections. Int. J. Earth Sci. 93, 659–682.
Murphy, J.B., Gutierrez-Alonso, G., Nance, R.D., Fernandez-Suarez, J., Keppie, J.D., Quesada, C., Strachan, R.A., Dostal, J., 2006. Origin of the Rheic Ocean: rifting along a Neoproterozoic suture? Geology 34, 325–328.
Nagata, T., 1961. Rock Magnetism. Maruzen, Tokyo, 350 pp.
Nance, R.D., Murphy, J.B., 1994. Constraining basement isotopic signatures and the palinspastic restoration of peripheral orogens: example from the Neoproterozoic Avalonian–Cadomian belt. Geology 22, 617–620.
Nance, R.D., Murphy, J.B., Strachan, R.A., D'Lemos, R.S., Taylor, G.K., 1991. Late Proterozoic tectonostratigraphic evolution of the Avalonian and Cadomian terranes. Precambrian Res. 53, 41–78.
Osozawa, S., Morimoto, J., Flower, M.F.J., 2009. "Block-in-matrix" fabrics that lack shearing but possess composite cleavage planes: a sedimentary mélange origin for the Yuwan accretionary complex in the Ryukyu island arc, Japan. Geol. Soc. Am. Bull. 121, 1190–1203.
Parés, J.M., van der Pluijm, B.A., 2002. Evaluating magnetic lineations (AMS) in deformed rocks. Tectonophysics 350, 283–298.
Passchier, C.W., Trouw, R.A.J., 2005. Microtectonics. Springer-Verlag, Berlin, 325 pp.
Patočka, F., Štorch, P., 2004. Evolution of geochemistry and depositional settings of Early Palaeozoic siliciclastics of the Barrandian (Teplá–Barrandian Unit, Bohemian Massif, Czech Republic). Int. J. Earth Sci. 93, 728–741.
Patočka, F., Pruner, P., Štorch, P., 2003. Palaeomagnetism and geochemistry of Early Palaeozoic rocks of the Barrandian (Teplá–Barrandian Unit, Bohemian Massif): palaeotectonic implications. Phys. Chem. Earth 28, 735–749.
Pin, C., Waldhausrová, J., 2007. Sm–Nd isotope and trace element study of Late Proterozoic metabasalts ("spilites") from the Central Barrandian domain (Bohemian Massif, Czech Republic). In: Linnemann, U., Nance, D., Kraft, P., Zulauf, G. (Eds.), The Evolution of the Rheic Ocean: From Avalonian–Cadomian Active Margin to Alleghenian–Variscan Collision. Geol. Soc. Am. Spec. Paper 423, pp. 231–247.
Pin, C., Kryza, R., Oberc-Dziedzic, T., Mazur, S., Turniak, K., Waldhausrová, J., 2007. The diversity and geodynamic significance of Late Cambrian (ca. 500 Ma) felsic anorogenic magmatism in the northern part of Bohemian Massif: a review based on Sm–Nd isotope and geochemical data. In: Linnemann, U., Nance, D., Kraft, P., Zulauf, G. (Eds.), The Evolution of the Rheic Ocean: From Avalonian–Cadomian Active Margin to Alleghenian–Variscan Collision. Geol. Soc. Am. Spec. Paper 423, pp. 209–229.
Platt, J.P., 1986. Dynamics of orogenic wedges and the uplift of high-pressure metamorphic rocks. Geol. Soc. Am. Bull. 97, 1037–1053.
Pouba, Z., Kříbek, B., 1986. Organic matter and the concentration of metals in Precambrian stratiform deposits of the Bohemian Massif. Precambrian Res. 33, 225–237.
Pouba, Z., Kříbek, B., Pudilová, M., 2000. Stromatolite-like cherts in the Barrandian Upper Proterozoic: a review. Bull. Czech Geol. Surv. 75, 285–296.
Powell, C.M., 1979. A morphological classification of rock cleavage. Tectonophysics 58, 21–34.
Röhlich, P., 1965. Geologische Probleme des mittelböhmischen Algonkiums. Geologie 14, 373–403.
Samson, S.D., D'Lemos, R.S., Miller, B.V., Hamilton, M.A., 2005. Neoproterozoic palaeogeography of the Cadomia and Avalon terranes: constraints from detrital zircon U–Pb ages. J. Geol. Soc. London 162, 65–71.
Sláma, J., Dunkley, D.J., Kachlík, V., Kusiak, M.A., 2008. Transition from island-arc to passive setting on the continental margin of Gondwana: U–Pb zircon dating of Neoproterozoic metaconglomerates from the SE margin of the Teplá–Barrandian Unit, Bohemian Massif. Tectonophysics 461, 44–59.
Štědrá, V., Kachlík, V., Kryza, R., 2002. Coronitic metagabbros of the Mariánské Lázně Complex and Teplá Crystalline Unit: inferences for the tectonometamorphic evolution of the western margin of the Teplá–Barrandian Unit, Bohemian Massif. In: Winchester, J.A., Pharaoh, T.C., Verniers, J. (Eds.), Palaeozoic amalgamation of Central Europe. Geol. Soc. London Spec. Publ. 201, pp. 217–237.
Štorch, P., 2006. Facies development, depositional settings and sequence stratigraphy across the Ordovician–Silurian boundary: a new perspective from the Barrandian area of the Czech Republic. Geol. J. 41, 163–192.
Strachan, R.A., Treloar, P.J., Brown, M., D'Lemos, R.S., 1989. Cadomian terrane tectonics and magmatism in the Armorican Massif. J. Geol. Soc. London 146, 423–426.
Suchý, V., Sýkorová, I., Melka, K., Filip, J., Machovič, V., 2007. Illite "crystallinity" maturation of organic matter and microstructural development associated with lowest-grade metamorphism of Neoproterozoic sediments in the Teplá–Barrandian unit, Czech Republic. Clay Miner. 42, 503–526.
Tait, J.A., Bachtadse, V., Franke, W., Soffel, H.C., 1997. Geodynamic evolution of the European Variscan fold belt: palaeomagnetic and geological constraints. Geol. Rundsch. 87, 585–598.
Tarling, D.H., Hrouda, F., 1993. The Magnetic Anisotropy of Rocks. Chapman and Hall, London, 217 pp.
Timmermann, H., Štědrá, V., Gerdes, A., Noble, S.R., Parrish, R.R., Dörr, W., 2004. The problem of dating high-pressure metamorphism: a U–Pb isotope and geochemical study on eclogites and related rocks of the Mariánské Lázně Complex, Czech Republic. J. Petrol. 45, 1311–1338.
Timmermann, H., Dörr, W., Krenn, E., Finger, F., Zulauf, G., 2006. Conventional and in situ geochronology of the Teplá crystalline unit, Bohemian Massif: implications for the processes involving monazite formation. Int. J. Earth Sci. 95, 629–647.
Tomek, Č., Dvořáková, V., Vrána, S., 1997. Geological interpretation of the 9HR and 503M seismic profiles in western Bohemia. In: Vrána, S., Štědrá, V. (Eds.), Geo-

logical Model of Western Bohemia Related to the KTB Borehole in Germany. J. Geol. Sci., Geol., vol. 47, pp. 43–50.
Torsvik, T.H., Cocks, L.R.M., 2004. Earth geography from 400 to 250 Ma: a palaeomagnetic, faunal and facies review. J. Geol. Soc. London 161, 555–572.
Treloar, P.J., Strachan, R.A., 1990. Cadomian strike-slip tectonics in NE Brittany. In: D'Lemos, R.S., Strachan, R.A., Topley, C.G. (Eds.), The Cadomian Orogeny, vol. 51. Geol. Soc. London Spec. Publ., pp. 151–168.
Venera, Z., Schulmann, K., Kröner, A., 2000. Intrusion within a transtensional tectonic domain: the Čistá granodiorite (Bohemian Massif)—structure and rheological modelling. J. Struct. Geol. 22, 1437–1454.
Vidal, P., Auvray, B., Charlot, R., Fediuk, F., Hameurt, J., Waldhausrová, J., 1975. Radiometric age of volcanics of the Cambrian "Křivoklát Rokycany" complex (Bohemian Massif). Geol. Rundsch. 64, 563–570.
von Raumer, J.F., Stampfli, G.M., 2008. The birth of the Rheic Ocean—Early Palaeozoic subsidence patterns and subsequent tectonic plate scenarios. Tectonophysics 461, 9–20.
von Raumer, J.F., Stampfli, G.M., Borel, G., Bussy, F., 2002. Organization of pre-Variscan basement areas at the north-Gondwanan margin. Int. J. Earth. Sci. 91, 35–52.
von Raumer, J.F., Stampfli, G.M., Bussy, F., 2003. Gondwana-derived microcontinents—the constituents of the Variscan and Alpine collisional orogens. Tectonophysics 365, 7–22.
Vrána, S., Štědrá, V. (Eds.), 1997. Geological model of western Bohemia related to the KTB borehole in Germany. J. Geol. Sci., Geol. 47, 240 pp.
Waldhausrová, J., 1966. The volcanites of the Křivoklát–Rokycany Zone. In: Fediuk, F., Fišera, M. (Eds.), Paleovolcanites of the Bohemian Massif, pp. 145–151.
Waldhausrová, J., 1971. The chemistry of the Cambrian volcanics in the Barrandian area. Krystalinikum 8, 45–75.
Waldhausrová, J., 1984. Proterozoic volcanics and intrusive rocks of the Jílové Zone (Central Bohemia). Krystalinikum 17, 77–97.
Winkler, A., Florindo, F., Sagnotti, L., 1996. Inverse to normal magnetic fabric transition in an upper Miocene marly sequence from Tuscany, Italy. Geophys. Res. Lett. 23, 909–912.
Worm, H.U., Clark, D., Dekkers, M.J., 1993. Magnetic susceptibility of pyrrhotite: grain size, field and frequency dependence. Geophys. J. Int. 114, 127–137.
Wortman, G.L., Samson, S.D., Hibbard, J.P., 2000. Precise U–Pb zircon constraints on the earliest magmatic history of the Carolina terrane. J. Geol. 108, 321–338.
Žák, J., Schulmann, K., Hrouda, F., 2005. Multiple magmatic fabrics in the Sázava pluton (Bohemian Massif, Czech Republic): a result of superposition of wrench-dominated regional transpression on final emplacement. J. Struct. Geol. 27, 805–822.
Zulauf, G., 1997. From very low-grade to eclogite-facies metamorphism: tilted crustal sections as a consequence of Cadomian and Variscan orogeny in the Teplá–Barrandian unit (Bohemian Massif). Geotekt. Forsch. 89, 1–302.
Zulauf, G., Dörr, W., Fiala, J., Vejnar, Z., 1997. Late Cadomian crustal tilting and Cambrian transtension in the Teplá–Barrandian unit (Bohemian Massif, Central European Variscides). Geol. Rundsch. 86, 571–587.
Zulauf, G., Schritter, F., Riegler, G., Finger, F., Fiala, J., Vejnar, Z., 1999. Age constraints on the Cadomian evolution of the Teplá–Barrandian unit (Bohemian Massif) through electron microprobe dating of metamorphic monazite. Zt. Deutsch. Geol. Ges. 180, 627–639.

5. Závěry

Předkládaná rigorózní práce shrnuje výsledky strukturního výzkumu v sz. části proterozoika tepelsko-barrandienské jednotky, která pravděpodobně představuje jeden z nejlépe zachovaných fragmentů akrečního prismatu v avalonsko–kadomském orogenním pásu, který se vyvinul podél severního aktivního okraje Gondwany během svrchního neoproterozoika. V centrální části TBJ byly vymapovány 3 litotektonické jednotky (sv.–jz. průběhu; Doména 1–3) oddělené křehkými zlomy a odlišující se litologií, stylem a intenzitou deformace, magnetické stavby a stupněm kadomské regionální metamotrfózy. Flyšoidní Doména 1 na SZ studované oblasti je doménou nejbližší předpokládanému oceánskému příkopu, která nebyla nikdy významně pohřbena a prodělala jen slabou deformaci a vrásnění. Centrální melanžová Doména 2 je charakteristická heterogenní intenzivní deformací v podmínkách nižší facie zelených břidlic a byla nasunuta k SZ přes doménu 1 podél zlomu upadajícímu k JV. V jv. části studované oblasti se nachází Doména 3, nejbližší vulkanickému oblouku a charakterizovaná monotónní litologií (převážují droby a břidlice), která byla pohřbena do hloubek odpovídajícím nižší facii zelených břidlic, kde byla přetištěna pervazívní k JV upadající kliváží a následně exhumována podél poklesového zlomu, upadajícímu k SZ. Tyto domény jsou interpretovány jako alochtonní tektonické šupiny, které byly různě pohřbeny a následně exhumovány z různých hloubek v akrečním prismatu během kadomské subdukce. Nasouvání Domény 2 přes Doménu 1 k SZ mohlo být způsobeno akrecí v čele prizmatu, zatímco k JV zapadající kliváž a exhumace domény 3 může zachycovat pervazívní zkracování během tektonického „podkládání“ a následnou horizontální extenzi zadní části prizmatu. Zlomy oddělující jednotlivé domény byly později reaktivovány během kambroordovické extenze a variské komprese. V porovnání s ostatními terány kadomského pásu, postrádá TBJ odkrytou prekadomskou kontinentální kůru, regionální horizontální posuny a zaobloukový magmatismus nebo LP–HT metamorfózu, což může být interpretováno

jako odraz kadomské subdukce pod nízkým úhlem. Naopak uvedené skutečnosti naznačují, že kadomská akreční prizmata se vyvíjela stejným způsobem jako ta moderní, což povyšuje TBJ na úroveň klíčové pozice pro pochopení stylu, kinematiky a časování akrečních procesů v avalonsko-kadomském pásu.